Reynolds Averaged Radiative Transfer Model

Carl A. Svoboda

School of Mathematical and Physical Sciences
Department of Mathematics and Statistics

This dissertation is for a joint MSc in the Departments of Mathematics & Meteorology and is submitted in partial fulfilment of the requirements for the degree of Master of Science

26 August 2011

Declaration

I confirm that this is my own work and the use of all material from other sources has been properly and fully acknowledged.

Signed .....

Acknowledgements

I would like to thank my supervisor Dr Robin Hogan for his continued dedication and support towards this preoject. I would also like to thank Dr Peter Sweby and the Natural Environment Research Council for giving me the opportunity and funding to undertake this MSc.

Abstract

In order for accurate predictions of climate change, it is essential that radiative transfer processes within the atmosphere are represented accurately in GCMs. The Radiative Transfer component of climate models is one of the 'rate-limiting' areas in the computation (Natraja *et al.*, 2005). While several techniques have been proposed to speed up radiative transfer calculations, they all suffer from accuracy considerations (Natraja *et al.*, 2005). A review of current techniques used within radiative transfer modelling is given followed by the development of a new, Reyolds averaged radiative transfer model. Starting with a simple case, reducing the radiative transfer equation (RTE) to exclude scattering and emission. The fluctuating terms within the RTE are Reynolds decomposed and a system of linear, homogeneous differential equations is solved involving a closure problem, which requires parameterization. Real atmospheric absortion spectra are used and an accuracy of 10^{-6} Wm^{-2} is achieved for 100 bands in an equal weighted band model, where each band has the same number of extinction coefficients within it. The models developed have difficulty in representing a large range of absorption coefficient. The next step in the development and testing of a Reynolds averaged radiative transfer model would be to include radiation travelling in different directions and to also include emission along the path, therefore having to include the Planck function. Then we would like to account for scattering. We would also like to account for an inhomogeneous path, where pressure and temperature change.

Contents

List of Figures

List of Tables

Chapter 1

Introduction

1.1 The General Problem

Global Climate Models (GCMs) are computationally expensive numerical models comprising of many components such as, Atmosphere, Ocean, Sea Ice, Land Surface models. They are often referred to as Earth Sytem Models. Currently GCMs can take months to produce predictions up to 100 years ahead. As more components are continuously being asdded to the GCM, such as Atmospheric Chemistry components, the amount of computational power required to run these models is increasing. Instead of waiting for computer technology to improve, we can look at existing code and attempt to find news numerical techniques to make the code more efficient (Dessler *et al.*, 2008).

In order for accurate predictions of climate change, it is essential that radiative transfer processes within the atmosphere are represented accurately in GCMs. Shortwave (SW) solar radiation is predominantly emitted from the Sun and Longwave (LW) radiation emitted from the Earth and atmosphere. LW Radiative transfer processes are the main force behind temperature changes, on climate scales, in the atmosphere and hence these processes play a major role in climate change (Liou, 1992). The processes that govern outgoing LW radiation (OLR) at the top of the atmosphere include the interaction of radiation between

gases and clouds. These processes have a strong impact on the surface energy balance (Ritter & Geleyn, 1992).

As in many areas of numerical modelling, especially in GCMs, it is desirable for the mathematics within the model to be calculated quickly, whilst describing as accurately as possible the interaction of radiative processes (Ritter & Geleyn, 1992) (Dessler *et al.*, 1996) as even a change of 1% in radiation calculations are significant for climate (Turner *et al.*, 2004).

At present, large computational resources are required for the calculation of radiative transfer in the atmosphere for weather and climate prediction (Fomin, 2004). The radiative transfer component of climate models is one of the 'rate-limiting' areas in the computation (Natraja *et al.*, 2005). While several techniques, which will be discussed later, have been proposed to speed up radiative transfer calculations, they all suffer from accuracy considerations (Natraja *et al.*, 2005). The need to improve the computational efficiency of the numerical models causes the problem of gaining the right balance between efficiency and accuracy (Stephens, 1984). Radiative transfer schemes will have to compromise between these two criteria (Ritter & Geleyn, 1992).

As full treatment of the radiative transfer code in GCMs, incorporating all known physics is computationally expensive, parameterization is required (Turner *et al.*, 2004). The cost effectiveness of a parameterization scheme is subject to many influences. First there is the solution method to the radiative transfer equation (RTE) and the approximation associated with it. Second there is the number of intervals used to resolve the spectrum. Further economy can be achieved in many models by considering only those optical constituents of the atmosphere that are important in a particular spectral domain. Often some atmospheric constituents in certain spectral intervals are neglected where their impact is well below that of other constituents (Ritter & Geleyn, 1992).

As an example of the importance in obtaining code accurate enough to model these atmospheric interactions, there are large differences among recent GCM simulations for prescribed changes in stratospheric water vapour (stratospheric water vapour being an important contributor to the observed stratospheric cool-

ing); this points to problems with the current GCM treatment of the absorption and emission by stratospheric water vapour (Oinas *et al.*, 2001).

Even considering the current computational efficiency of radiation calculations in numerical weather prediction models and GCMs, these models still require substantial computational time relative to all other physical and dynamical calculations. As a result, radiation subroutines in these models are usually not called as often as would be desired, even being called less often than the time scale on which clouds evolve in the models. High spectral accuracy is therefore usually achieved at the expense of poor temporal resolution, with the radiation scheme often only called every three hours, which can lead to errors in the diurnal cycle and change the climate sensitivity of the model (Pawlak *et al.*, 2004). If the number of calculations could be further reduced, the savings in computational time could be used to call the radiation subroutines on a time scale that would allow a more realistic interaction between radiation and clouds (Pawlak *et al.*, 2004).

Although computer power is continuously being developed and the time taken to run GCMs is reducing, one cannot simply wait for the extra power to become available as more and more components to the climate change model are continually being developed and coupled to GCMs. In order to speed up the numerical computation of these models it is therefore essential that existing code is reviewed and improved.

1.2 Aims

As current methods for radiative transfer calculations still constitute a significant fraction of the cost of a GCM, the aim of this project is to investigate the credentials of a new numerical scheme for calcualting long wave transmission and heating reates in the atmosphere, which could further improve the computatiaonal efficiency and time taken to run radiative transfer codes in atmospehric models. This new model will aim to explore the potential in using the radiative

transfer equation and applying Reynolds averaging to the variables which vary with wavelength. The main aims will be:

- Determine the accuracy of a simplified situation, no scattering or emission and with radiation travelling in only one direction.
- Investigate how the standard deviation, σ of the absorption coefficients affects the accuracy of the scheme
- Investigate the number of quadtratue points required to acheive desired accuracy
- Investigate if bands are bands still required

  Total number of bands

  How best to define the bands
- Add emmission, planck function into equations
- A diffusivity fator, for radiation travelling in different directions

Chapter two will give an overview of the science background required to fully understand the processes within the model. Chapter three gives a summary of current techniques used to treat the complicated absorption spectrum. Chapter four gives the derivation of the equations used within the model and a description of how the model works. Chapter five presents some results from the model and chapter six discusses these results.

Chapter 2

Scientific Background

The radiative transfer process is essentially the process of interactions between matter and a radiation field (Fu & Liou, 1992). Thermal Infra Red (IR) radiation is the most important factor when considering the distribution of heat within the atmosphere. IR radiation is emitted from the Earth and the atmosphere. The IR part of the electromagnetic spectrum covers wavelengths from 0.7 μm up to 1000 μm. The IR band is often divided into three further bands: the near IR, the thermal IR and the far IR (Petty, 2004). Over 99% of the energy emitted by the Earth and the atmosphere is located within the theral IR band (4 μm - 50 μm) (Petty, 2004). Radiation within this band will be referred to as longwave (LW) radiation. Energy emitted in the other IR bands is essentially irrelevant for the atmospheric energy budget. The state of the Earth's atmosphere is heavily dependent on the interactions of LW radiation with the atmosphere. These interactions may be classified as absorption, scattering or emission, all of which depend on the composition of the atmosphere with regards to gases, clouds and other particles such as suit or dust.

As the Earth's surface absorbs the incoming, short wave (SW) solar radiation and emits the LW IR radiation, it is predominantly the amount of thermal IR radiation which is able to escape back into space which determines the overall net energy balance (the difference between incoming solar radiation and outgoing long wave radiation) at the top of the atmosphere and subsequently the average

temperature of the Earth's atmosphere. Hence IR radiation and the amounts absorbed and re-emitted within the atmosphere play a major role in quantifying future climate change (Liou, 1992).

2.1 Emission

The Earth and the atmosphere are continuously emitting IR radiation which may be radiated out into space or may be absorbed by other parts of the atmosphere. The emission of an object is directly related to the temperature of that object. An object of temperature T will emit over all possible wavelengths. The relationship between, temperature, wavelength λ and the amount of radiation emitted is defined by the Planck Function (2.1) (Petty, 2004):

$$B_\lambda(T) = \frac{2hc^2}{\lambda^5(e^{hc/k_B\lambda T} - 1)}, \tag{2.1}$$

where c=2.988×10^8 m s^{-1}, (the speed of light), h=6.626×10^{-34} J s represents Planck's constant and k_B=1.381×10^{-23} J K^{-1} represents the Boltzmann's constant.

Figure (2.1) shows the shape of the Planck Function for several atmospheric temperatures. The curves describe the maximum amount of thermal radiation a body could emit, thus describing a 'black body' (one which absorbs and emits all radiation incident upon it) (Petty, 2004).

For any temperature there will be a specific wavelength at which there occurs a maximum in the amount of radiation emitted. This wavelength is defined by Wien's Displacement Law (2.2) (Petty, 2004):

$$\lambda_{max} = \frac{C}{T}, \tag{2.2}$$

where λ_{max} is the wavelength at which the peak in emission occurs and C=2897 μm K.

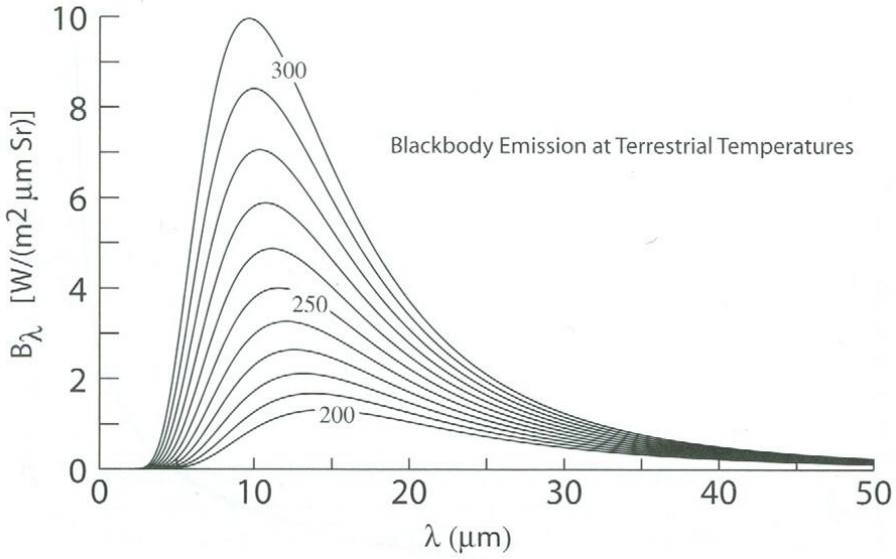

Figure 2.1: The Planck Function B_λ for Blackbodies at typical atmospheric temperatures (Petty, 2004).

Equation (2.2) shows that the warmer the object, the shorter the wavelength at which the peak in emission occurs. If Planck's Function is integrated over all wavelengths we obtain Stefan-Boltzmann Law (2.4), which quantifies the total amount of radiation which can be emitted from a perfect black body (the blackbody flux F_{BB}) (Petty, 2004):

$$F_{BB}(T) = \pi \int_0^\infty B_\lambda(T) d\lambda, \tag{2.3}$$

$$F_{BB}(T) = \sigma T^4, \tag{2.4}$$

where $\sigma = 5.67 \times 10^{-8}$ $\mathrm{Wm^{-2}K^{-4}}$.

2.2 Absorption and Scattering

We can define the extinction coefficient β_e (2.5) as the sum of the extinction due to absorption β_a and the extinction due to scattering β_s (Petty, 2004).

$$\beta_e = \beta_a + \beta_s. \tag{2.5}$$

We are now able to define the single scatter albedo $\tilde{\omega}$ (2.6), which defines the relative importance of scattering and absorption. $\tilde{\omega}$ ranges from 0 for purely absorbing mediums to 1 for purely scattering material (Petty, 2004):

$$\tilde{\omega} = \frac{\beta_s}{\beta_e}. \tag{2.6}$$

All the constituents of the atmosphere have unique absorption spectrum in the IR band. In a cloud-free atmosphere, the overall outgoing LW radiation is predominantly determined by the absorbing gases. Where absorption is strongest, the transmittance is weakest. The main absorbing gases of the atmosphere and the wavelength ranges over which they absorb can be deduced from figure (2.2). It also shows the total transmittance of the entire atmosphere. The total transmittance due to all the constituents is simply the product of the transmittances due to the individual constituents.

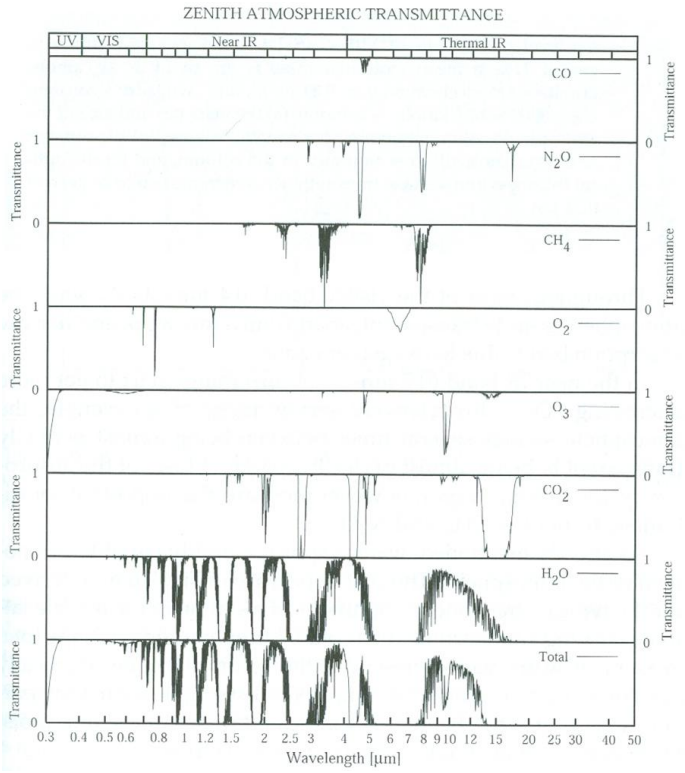

Figure 2.2: The zenith transmittance of a cloud and aerosol free atmosphere for a mid latitude summertime. The bottom panel depicts the combined effect of all the constituents above (Petty, 2004).

The most important absorbers are carbon dioxide (CO_2), water vapour (H_2O), ozone (O_3), methane (CH_4) and nitrous oxide (N_2O) (Liou, 1992). All these constituents are triatomic molecules and therefore have complicated absorption spectra due to rotational and vibrational transitions. In the thermal IR band, there is strong absorption by CO_2 around 4 μm and around 15 μm and water vapour has a strong absorption band between 5-8 μm. Ozone has a strong absorption band around 9.6 μm and is also important in all parts of the of the spectrum, except the IR window. Between 8-13 μm, the atmosphere is relatively transparent. This part of the spectrum is termed 'the atmospheric window'.

Water vapour is the most important absorber in the IR band. Figure (2.3) depicts the zenith transmittance when only water vapour is considered.

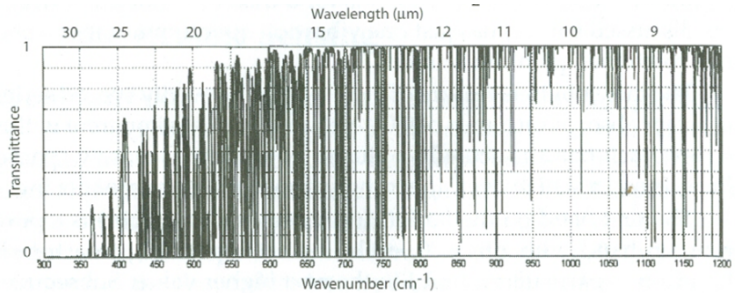

Figure 2.3: The zenith transmittance of the atmosphere due to water vapour in the thermal IR (Petty, 2004).

The x-axis is measured in wavenumber $\tilde{v}$, which is simply the reciprocal of the wavelength (2.7) and therefore its units are in cm^{-1}.

$$\tilde{v} = \frac{1}{\lambda}. \tag{2.7}$$

The absorption spectrum of water vapour exhibits great complexity and if one were to zoom in on figure (2.3), it would become apparent that the complexity exists on wave length scales up to 10^{-4} cm^{-1}. At wavelengths greater than 25 μm the atmosphere is more or less opaque with regards to H_2O absorption (Liou, 1992).

2.3 Radiative Transfer Equation

We are interested in the amount of radiation travelling through a part of the atmosphere. As the electromagnetic (EM) radiation transports energy, we quantify the amount of radiation transferred with power, using the Watt, W (the amount of energy measured in Joules, J, per unit time, s) (Petty, 2004). It is common to refer to the amount of radiation received in terms of its flux density F, the rate of energy transfer per unit area Wm^{-2}. From here on in flux shall be used to refer to flux density. The flux is the rate at which the radiation passes through a flat surface including all wavelengths between a specified range (Petty, 2004).

We shall consider how EM radiation is effected when it travels along a path of homogeneous medium and is able to be absorbed by the medium. The intensity or radiance tells us about the strength and direction of the various sources which contribute to the flux.

The flux passing through the surface will be the integral of intensity over all the possible directions from which the radiation is incident. As only one direction is normal to the surface, all contributions from other directions must be weighted by the cosine of the incident angle relative to the normal. So in spherical polar coordinates the relationship between flux and intensity can be written (Petty, 2004),

$$F = \int_0^{2\pi} \int_0^{\pi/2} I(\theta, \psi) \cos\theta \sin\theta d\theta d\psi, \tag{2.8}$$

where $I(\theta, \psi)$ is the irradiance over all possible incident angles. We shall now consider the absorption of a monochromatic EM wave propagating through a homogeneous atmosphere. The most simple governing equation for this occurs where the wave is travelling in one direction only and is attenuated only by absorption (Petty, 2004),

$$dI_\lambda(z) = -\beta_a I_{\lambda,0} dz, \tag{2.9}$$

where β_a is the absorption coefficient, which depends on the physical medium and the wavelength of the radiation, $\mathrm{I}_\lambda(z)$ is the intensity of the transmitted radiation at some distance, z, and $\mathrm{I}_{\lambda,0}$ is the intensity of the radiation at z=0. We can rearrange and integrate (2.9) over the range of intensities and the distance the radiation travels to obtain (Petty, 2004):

$$I_\lambda = I_{\lambda,0} \exp(-\beta_a z). \tag{2.10}$$

This shows that in the homogeneous absorbing atmosphere the intensity of the radiation falls off exponentially with distance. There are a few factors that would need to be considered to make this approximation more realistic for the

atmosphere. The beam of radiation is not only attenuated by absorption, but also by scattering due to interactions with particles. We can now use our previously defined extinction coefficient in place of the absorption coefficient to account for scattering. We consider our beam of radiation over a finite path where extinction coefficient varies with location. We replace the height, z, by s to represent a distance in any direction, represented by fig. (2.4).

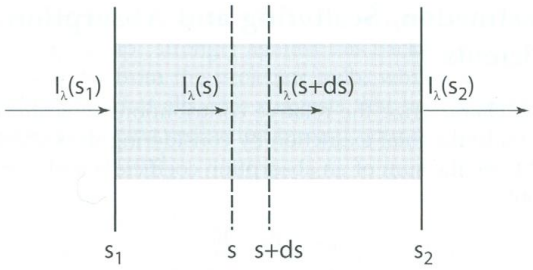

Figure 2.4: Depletion of radiation over an infinitesimal path ds (Petty, 2004)

If ds is considered to be infinitesimal, then the extinction coefficient β_e will be constant within the interval. The radiation will then change by an infinitesimal amount dI_λ and we can re-write (2.9) to include loss due to scattering, however no gain from scattering:

$$dI_\lambda(s) = -I_\lambda(s)\beta_e(s)ds. \tag{2.11}$$

We can consider the amount of radiation attenuated due to absorption only by writing (2.12) (Petty, 2004)

$$dI_{abs} = -I\beta_a ds. \tag{2.12}$$

Neglecting scattering ($\beta_a = \beta_e$), we know from Kirchoff's law discussed earlier that the absorptivity of any material is equal to the emissivity of that material. We can therefore define the amount of radiation that the thin layer of air will

emit by (2.13) (Petty, 2004):

$$dI_{emit} = B_\lambda(T)\beta_a ds, \tag{2.13}$$

enabling us to define Schwarzschild's Equation (2.14), the net change in radiation over the infinitesimal path in a non scattering medium (Petty, 2004):

$$dI = dI_{abs} + dI_{emit} = \beta_a(B - I)ds. \tag{2.14}$$

We are now ready to include scattering into our radiative transfer equation. Now we have

$$dI_{ext} = -\beta_{ext} I ds. \tag{2.15}$$

We must consider one more process to complete the RTE, in considering a new source term which includes the contributions to the beam as a result of scattering from other directions. We shall call this new source term, dI_{scat}. This term will be proportional to the scattering coefficient β_s. We can define the direction of travel we are interested in $\hat{\mathbf{\Omega}}$ and we can state that any radiation from any direction (defined by $\hat{\mathbf{\Omega}}'$)could contribute to $\hat{\mathbf{\Omega}}$. The contributions from all directions will sum linearly. We can therefore denote dI_{scat} by integrating over the whole solid angle and by defining the phase function $\mathrm{p}(\hat{\mathbf{\Omega}}', \hat{\mathbf{\Omega}})$ (Petty, 2004).

$$dI_{scat} = \frac{\beta_s}{4\pi} \int_{4\pi} p(\hat{\mathbf{\Omega}}', \hat{\mathbf{\Omega}}) \mathbf{I}(\hat{\mathbf{\Omega}}') \mathbf{d}\omega' \mathbf{ds}. \tag{2.16}$$

Our change in radiation dI is now made up of three terms:

$$dI = dI_{ext} + dI_{abs} + dI_{scat}. \tag{2.17}$$

We can divide through by the change in optical thickness dτ and can then write the complete form of the RTE (2.18) (Petty, 2004)

$$\frac{dI(\hat{\mathbf{\Omega}})}{d\tau} = -I(\hat{\mathbf{\Omega}}) + (\mathbf{1} - \tilde{\omega})\mathbf{B} + \frac{\tilde{\omega}}{\mathbf{4}\pi}\int_{\mathbf{4}\pi} \mathbf{p}(\hat{\mathbf{\Omega}}', \hat{\mathbf{\Omega}})\mathbf{I}(\hat{\mathbf{\Omega}}')\mathbf{d}\omega'. \tag{2.18}$$

2.4 Reynolds Decomposition

Figure (2.3) of the absorption spectrum for water vapour in the thermal IR is very remeniscent of a turbulence spectrum observed in many other areas of the atmosphere, such as the variation in surface wind speed over a certain amount of time. The transmittance due to water vapour appears to vary randomly across wavelengths, however the ability to find a mean value suggests that the spectrum is not random.

We can average the transmittance spectrum over a certain, number of intervals, averaging out the positive and negative fluctuatios about the mean. The mean transmittance in one interval is denoted, $\overline{\mathrm{T}}$. At any one particular wavelength, we can subtract $\overline{\mathrm{T}}$ from the actual transmittance, T, which will result in the fluctuating part, T$'$. This is represented schematically in figure (2.5) which shows an expanded view of a spectrum. The fluctuating part is seen to be the difference between the actual transmittance and the mean transmittance. From the graph it is clear that T$'$ can be positive and negative (Stull, 1989).

This process is known as Reynolds Averaging and we can write the transmittance for a given wavelength as the mean transmittance plus its respective fluctuating part,

$$T = \overline{T} + T'. \tag{2.19}$$

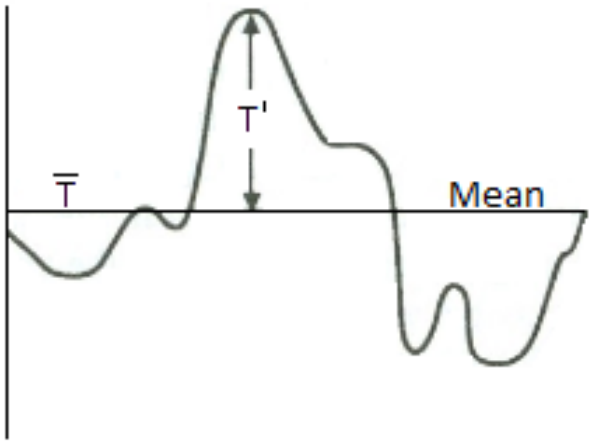

Figure 2.5: The deviation, T′ of the actual, transmittance, T, from the local mean, $\overline{\mathrm{T}}$

2.5 Reynolds Averaging Rules

If we let A and B be two variables that are dependent on the wavelength. We can show some rules using integration.

2.5.1 Rule One

The average of a sum (Stull, 1989):

$$\overline{\mathrm{A}+\mathrm{B}} = \frac{1}{\lambda_N}\int_{\lambda=0}^{\lambda_N}(\mathrm{A}+\mathrm{B})\,\mathrm{d}\lambda \tag{2.20}$$

$$= \frac{1}{\lambda_N}\left(\int_{\lambda}\mathrm{A}\,\mathrm{d}\lambda+\int_{\lambda}\mathrm{B}\,\mathrm{d}\lambda\right) \tag{2.21}$$

$$= \frac{1}{\lambda_N}\int_{\lambda}\mathrm{A}\,\mathrm{d}\lambda+\frac{1}{\lambda_N}\int_{\lambda}\mathrm{B}\,\mathrm{d}\lambda \tag{2.22}$$

$$= \overline{\mathrm{A}}+\overline{\mathrm{B}} \tag{2.23}$$

2.5.2 Rule Two

An average value acts as a constant, when averaged a second time over the same wavelength interval (Stull, 1989).

$$\frac{1}{\lambda_N}\int_{\lambda=0}^{\lambda_N} \mathrm{A}\,\mathrm{d}\lambda = \overline{\mathrm{A}} \tag{2.24}$$

$$\frac{1}{\lambda_N}\int_{\lambda=0}^{\lambda_N} \overline{\mathrm{A}}\,\mathrm{d}\lambda = \overline{\mathrm{A}}\,\frac{1}{\lambda_N}\int_{\lambda=0}^{\lambda_N} \mathrm{d}\lambda \tag{2.25}$$

$$= \overline{\mathrm{A}} \tag{2.26}$$

$$\overline{(\overline{\mathrm{A}})} = \overline{\mathrm{A}} \tag{2.27}$$

Similarly we can deduce,

$$\overline{(\overline{\mathrm{A}}\,\mathrm{B})} = \overline{\mathrm{A}}\,\overline{\mathrm{B}}. \tag{2.28}$$

2.5.3 Rule Three

$$\left(\overline{\frac{\mathrm{dA}}{\mathrm{d}z}}\right) = \frac{\mathrm{d}\overline{\mathrm{A}}}{\mathrm{d}z}. \tag{2.29}$$

2.5.4 Rule Four

The above three rules can be used to help us understand further rules when the variables are split into mean and fluctuating parts e.g. $\mathrm{A} = \overline{\mathrm{A}} + \mathrm{A}'$ (Stull, 1989)

$$\overline{\mathrm{A}} = \overline{\left(\overline{\mathrm{A}} + \mathrm{A}'\right)} \tag{2.30}$$

$$= \overline{(\overline{\mathrm{A}})} + \overline{\mathrm{A}'} \tag{2.31}$$

$$= \overline{\mathrm{A}} + \overline{\mathrm{A}'} \tag{2.32}$$

The only way the above can be true is if,

$$\overline{\mathrm{A}'} = 0. \tag{2.33}$$

This makes sense as the sum of the positive deviations from the mean must equal the sum of the negative deviations from the mean.

2.5.5 Rule Five

If we begin with the product $\overline{\mathrm{A}}\,\mathrm{B}'$ and find its average, we use the above rules to deduce (Stull, 1989),

$$\begin{aligned}
\overline{\overline{\mathrm{A}}\,\mathrm{B}'} &= \overline{\mathrm{A}}\,\overline{\mathrm{B}'} && (2.34)\\
&= \overline{\mathrm{A}} \times 0 && (2.35)\\
&= 0 && (2.36)
\end{aligned}$$

2.5.6 Rule Six

The average of the product of A and B is (Stull, 1989):

$$\begin{aligned}
\overline{(\mathrm{A} \times \mathrm{B})} &= \overline{\left(\overline{\mathrm{A}} + \mathrm{A}'\right)\left(\overline{\mathrm{B}} + \mathrm{B}'\right)} && (2.37)\\
&= \overline{\left(\overline{\mathrm{A}}\,\overline{\mathrm{B}} + \mathrm{A}'\,\overline{\mathrm{B}} + \overline{\mathrm{A}}\,\mathrm{B}' + \mathrm{A}'\,\mathrm{B}'\right)} && (2.38)\\
&= \overline{\left(\overline{\mathrm{A}}\,\overline{\mathrm{B}}\right)} + \overline{\left(\mathrm{A}'\,\overline{\mathrm{B}}\right)} + \overline{\left(\overline{\mathrm{A}}\,\mathrm{B}'\right)} + \overline{\left(\mathrm{A}'\,\mathrm{B}'\right)} && (2.39)\\
&= \overline{\mathrm{A}}\,\overline{\mathrm{B}} + 0 + 0 + \mathrm{A}'\,\mathrm{B}' && (2.40)\\
&= \overline{\mathrm{A}}\,\overline{\mathrm{B}} + \overline{\mathrm{A}'\,\mathrm{B}'} && (2.41)
\end{aligned}$$

The nonlinear term $\overline{\mathrm{A}'\,\mathrm{B}'}$ must be retained.

Chapter 3

Literature Review

As already seen, atmospheric gases have absorption coefficients that vary rapidly as a function of wavelength λ or wave number v, often changing by several orders of magnitude across the electromagnetic spectrum (Petty, 2004). This provides a great problem when the absorption spectra are modelled in GCMs, as there can be O(10^5) individual absorption lines within the spectrum. If we were to model each individual line, large amounts of computer power would be required to calculate the fluxes in the atmosphere (Ellingson *et al.*, 1991). Here we shall discuss some of the techniques developed to overcome this problem and reduce the time taken for the models to run, increasing the computational efficiency, whilst attempting to maintain a suitable degree of accuracy.

3.1 Line by Line Calculations

Absorption occurring at the smallest scale, that of the line, is described by the Lorenz line absorption profile. The most straightforward and accurate but most computationally expensive way to perform radiative transfer calculations is to divide the full spectrum into monochromatic (one wavelength) intervals, or sufficiently small so as to be treated as monochromatic (10^{-4} to 10^{-2} cm^{-1}) (Ellingson *et al.*, 1991). The relative contributions of all relevant absorption lines (all lines whose wings contribute to important absorption at a particular wavelength)

are summed to the absorption coefficient, β_a, for the wave number in question (Petty, 2004). Integrating over all intervals in the spectrum then provides fluxes and heating rates (Ellingson *et al.*, 1991). This however is not a simple task. The absorption spectrum depends on many things, including the location, strengths and shapes of the spectral lines (Ellingson *et al.*, 1991).

A LBL calculation of the average transmittance of a spectral interval $(v_1 - v_2)$ over a finite mass path, u, can be calculated by considering (Petty, 2004):

$$T(u) = \frac{1}{v_2 - v_1} \int_{v_1}^{v_2} \exp[-k(v)u]dv, \tag{3.1}$$

which can be approximated as a sum:

$$T(u) = \sum_{i=1}^{N} \alpha_i \exp[-k(v)u], \tag{3.2}$$

where N is the number of frequencies, v_i, where $k(v)$ is evaluated and α_i are weighting coefficients depending on the quadtrature method used.

Because the technique involves summing the contributions from each spectral line, it is referred to as the Line-By-Line technique (LBL) (Ellingson *et al.*, 1991). If this approach was to be used to calculate heating rates in the atmosphere, the monochromatic calculation would need to be repeated for a large number of wavenumbers as well as at a number of altitudes (Petty, 2004). This means that radiative heating calculations potentially require millions of calculations to obtain a suitable accuracy (Pawlak *et al.*, 2004). Where field measurements are unavailable, LBL techniques provide the best benchmark for analysis of other numerical methods (Ellingson *et al.*, 1991). Using this approach with current computer technology would mean a GCM would take longer than a decade to produce a prediction a decade into the future it is therefore not suitable for calculations in climate models (Petty, 2004). One model which is extensively used to compare against other numerical radiation codes is the Line-By-Line Radiative Transfer Model developed by (Clough et al. 1992) (LBLRTM).

3.2 Band Models

Due to the difficulty and computational demands of treating a single Lorenz line individually, the idea of the band model was developed, which enables certain characteristics of the band to be determined using simple statistical relationships, such as, averaging of the absorption properties (Petty, 2004). An analytic approximation for the transmittance is then derived. (Stephens, 1984) suggests that the most widely used in atmospheric flux calculations is that of Goody (1952) where the absorbing lines are assumed to be randomly distributed.

Narrow band models (NBM) get their name by the process of dividing the spectrum into a number of small intervals which are small enough to regard the Planck function as constant across that interval. The interval must also be wide enough to be able to smooth the variation in the spectrum (Stephens, 1984). Wide band models (WBM) require the use of LBL or NBM models to construct models using larger bands, sometimes over the whole spectrum (Stephens, 1984).

When defining the characteristics within the band there are some considerations which are important:

- The spacing between the lines to be considered, $\partial = \Delta v/N$, where N is the number of lines in a certain spectral interval
- How the lines being considered are distributed within the spectral interval. There are two main choices: random and regular (periodic). The former may be an appropriate description of parts of the water vapour spectrum. The latter might be more suited to some regions in the CO_2 spectrum. This is important as the distribution choice will determine how many lines present will overlap other lines. This overlap is reduced in a regular distribution
- The individual line widths. These are typically treated as constant for all the lines
- The distribution and range of the strengths of the lines.

3.3 k-distribution Method

3.3.1 k-distribution Method Theory

This method was first discussed by Ambartzumin (1936). It aims to perform the radiative calculations with larger discretisations by replacing the complex integration over wavenumber with an equivalent integration over a much smoother function (Petty, 2004) and involves grouping spectral intervals according to absorption coefficient strength (Natraja *et al.*, 2005). The absorption coefficient across a portion of the spectrum can be reordered into a monotonically increasing function called the k-distribution function (Modest & Zhang, 2002).

When the k-distribution method is used within a narrow band model, the longwave spectrum $k(v)$, is divided into N intervals Δv_i, each having a smaller range of $k(v)$ values (Mlawer *et al.*, 1995). This procedure treats each subinterval in an equivalent manner as a spectral point is treated in a monochromatic radiative transfer method (Mlawer *et al.*, 1997). The division of these intervals is determined by the fact that they must be large enough to contain a significant amount of absorption lines associated with a particular absorber and also, they must be small enough so that the Planck function $B_v(T)$ can be treated as constant and equal to $\overline{B}_i$ across the band (Petty, 2004). The creation of the k-distribution involves assigning each absorption coefficient $k(v)$ a value g (0-1) that represents the fraction of the absorption coefficients in the band smaller than the representative $k(v)$. The k-values are re-arranged into ascending order transforming the spectrum into a smooth monotonically increasing function of the absorption coefficient, representing a cumulative k-distribution, g, defining a mapping, v - g (Mlawer *et al.*, 1995). This can be seen in figure (3.1), which shows one such mapping, where the absorption coefficients for the spectral range (30-700 cm^{-1}) undergo a transformation into g-space figure (3.1b). The effect of this reordering is simply a rearrangement of the sequence of terms in the integral over wavenumber in the radiative transfer equations (Mlawer *et al.*, 1997).

By integrating over $k(g)$ instead of the complicated $k(v)$ we can replace the

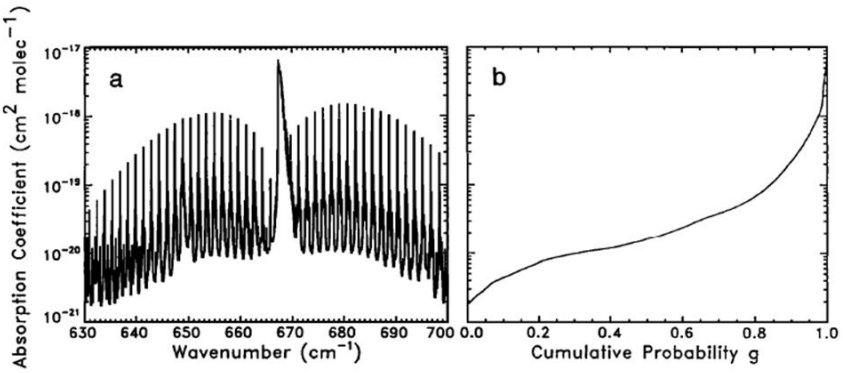

Figure 3.1: Absorption coefficients due to carbon dioxide for a layer (P = 507 mbar) in the mid latitude Summer atmosphere for the spectral range (30-700 cm^{-1}) (a) as a function of wavenumber and (b) after being rearranged in ascending order taken from (Mlawer *et al.*, 1997).

integral in (3.1) with (Petty, 2004)

$$T(u) = \int_0^1 \exp[-k(g)u]dg. \tag{3.3}$$

Now, instead of requiring O(10^5) calculations to cover the spectrum in flux and heating rate calculations, the cumulative k-distribution can be integrated with only a few quadrature points due to its smoothness. The k-distribution method is exact for a homogeneous atmosphere (Pawlak *et al.*, 2004).

3.3.2 k-distribution Method Limitations

A limitation of the k-distribution method is that the Planck function must be nearly constant over the spectral interval of interest (e.g., Goody and Yung 1989). Although the Planck function varies smoothly, it covers a range of several orders of magnitude across the spectrum. In radiative transfer calculations, k-distributions are therefore constructed for a number of smaller spectral bands over which the Planck function varies less (Pawlak *et al.*, 2004).

3.4 Correlated k-distribution Method

3.4.1 Correlated k theory

The k-distribution method discussed above assumes a homogeneous path (one over which the temperature and pressure remain the same). This means the method would only suit very short paths through the atmosphere. This led to an extension of the k-distribution method to account for vertical paths in the function where the temperature and pressure vary (Petty, 2004).

This extension to the k-distribution method is the correlated k-distribution method (CKD), first discussed by Lacis et al (1979). The vertical non-homogeneity of the atmosphere is accounted for by assuming a simple correlation of the k-distributions at different temperatures and pressures for a given gas (Fu & Liou, 1992). The k-distribution in a given layer is assumed to be fully correlated with the k-distribution in the next layer (Mlawer *et al.*, 1997). This means that the absorption coefficient in a spectral interval at one atmospheric level has the same relative position in the cumulative k-distribution as the absorption coefficients in the same spectral interval at every other level. Figure (3.2) shows how the process described above.

What remains to be done is to solve the RTE for a small number of absorption coefficients k(g). In the correlated-k approach this is generally done by Gaussian quadrature, since this gives a high degree of accuracy with relatively few RTE evaluations. The most primitive and least accurate quadrature scheme would be the use of the trapezoidal rule (Modest & Zhang, 2002) which is commonly known as the Weighted Sum of Gray Gases WSGG Method (Jacobson, 2004). The resulting radiances, weighted by the sizes of their respective intervals, can then be summed to yield the total radiance for the spectral band (Mlawer *et al.*, 1995)

We can define an applicable equation for the transmittance across an inho-

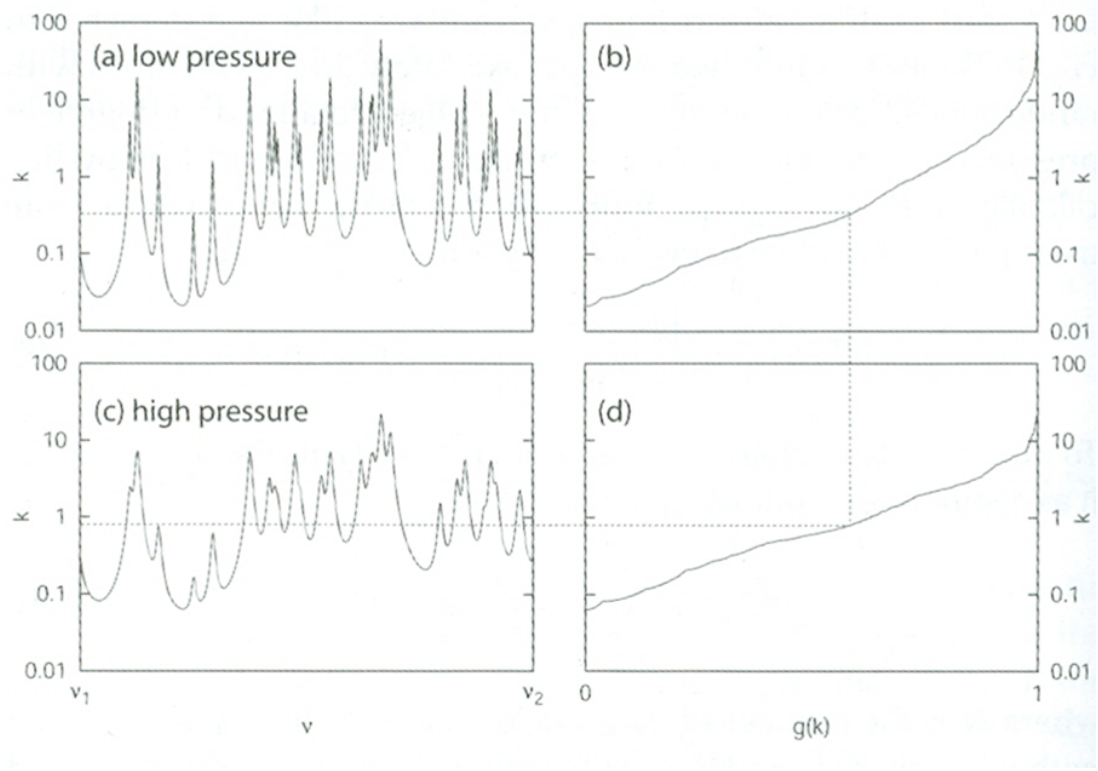

Figure 3.2: The k-distribution method and its extension to the correlated k method. (a) Absorption spectrum at low pressure, (b) sorting k to increase monotonically to form the function $g(k)$. (c) the same as for a and b, however at higher pressure, so are effected by pressure broadening (Petty, 2004)

mogeneous path (Petty, 2004).

$$T(u) = \int_0^1 \exp\left[-\int_0^u k(g,u')du'\right] dg. \tag{3.4}$$

This equation calculates the transmittance for a specific value of g over the path, from the current location $u' = 0$ and another location $u' = u$. These transmittances are then averaged over the interval 0<g<1 to obtain the band transmittance.

The correlated-k method is based on the fact that inside a spectral band, which is sufficiently narrow to assume a constant Planck function, the precise knowledge of each line position is not required for the computation (Modest & Zhang, 2002). It is an approximate technique for the accelerated calculation of fluxes and cooling rates for inhomogeneous atmospheres. It is capable of achieving an accuracy comparable with that of LBL models with an extreme reduction in the number of radiative transfer operations performed (Mlawer *et al.*, 1997).

Correlated-k models generally have either sacrificed accuracy to preserve computational or have maintained model accuracy but with a dramatically increased number of operations to compute the needed optical depths (Mlawer *et al.*, 1997).

3.4.2 Correlated k Limitations

The process described above, presents a problem. The drawback of the correlated k-distribution method is that it assumes that atmospheric optical properties are correlated at all points along the optical path, such that spectral intervals with similar optical properties at one level of the atmosphere will remain similar at all other levels (Natraja *et al.*, 2005). Although this assumption is valid for homogeneous atmospheres it usually breaks down for realistic inhomogeneous atmospheres and therefore introduces some error. $k(g)$ actually varies with altitude, pressure, temperature, and relative molecular concentrations change from layer to layer (Jacobson, 2004). Any given value of k can be associated with many

different frequencies. This can be seen in (3.2), the horizontal dotted line corresponds to a single value of k, yet has many values of frequency associated with it. In the CK Method, the absorption coefficient at all of these frequencies is associated to a single value of g (depicted by the intersection of the dotted line with the $k(g)$ curve figure (3.2b)).

Figure (3.2c) shows the absorption spectrum for a level higher in the atmosphere and its corresponding $k(g)$ mapping is represented in figure (3.2d). The absorption spectrum is affected by pressure broadening leading to a smoother spectrum with less extreme values of k. As a result, the spectral elements that contribute to a subinterval of the k-distribution for one homogeneous layer will not be mapped to the corresponding subinterval for a different atmospheric layer (Mlawer *et al.*, 1997). This leads to a different $k(g)$ distribution at the higher pressure. The newly determined frequencies at higher pressure, determined by the choice of k at lower pressure are not far off those frequencies at the lower pressure and this method does provide results within accuracy restraints.

The CKD method overestimates and underestimates the absorption in the vicinity of maximum and minima respectively. As a result, the CKD method may overestimate the spectral mean transmittance, leading to a more transparent atmosphere (Fu & Liou, 1992). The method does calculate fluxes and heating rates to errors of less than 1% (Petty, 2004) and is three orders of magnitude less computational power is required than LBL calculations (Petty, 2004).

3.5 Rapid Radiative Transfer Model (RRTM)

RRTM stands for the Rapid Radiative Transfer Model (Clough *et al.*, 2005). Modelled molecular absorbers are water vapour, carbon dioxide, ozone, nitrous oxide, methane, oxygen, nitrogen, and halocarbons. The model is accurate and fast, using the correlated-k method in its computation. RRTM divides the LW spectral region into 16 bands chosen for their homogeneity and radiative transfer properties (Mlawer *et al.*, 1995) (Clough *et al.*, 2005). There are a number of areas which can be explored to improve the speed of the model. The number

of subintervals into which some of the bands are divided could be reduced and combining separate spectral regions which have similar absorbing properties into single spectral bands could help reduce the time taken for the model to run (Mlawer *et al.*, 1997).

(Fu & Liou, 1992) explored the optimum number of g values suitable within each band. They found that the number of quadrature points to provide sufficient accuracy could vary from 1 (for weak absorbing bands) to 10 (for strong absorption bands).

Each spectral band in the RRTM is broken into 16 intervals with 7 intervals lying between $g = 0.98$ and $g = 1.0$. This modified quadrature spacing is done to better determine the cooling rate where high values of $k(g)$ are associated with the centres of the spectral lines in the band (Mlawer *et al.*, 1995). The k-distribution is divided into subintervals of decreasing size with respect to g, with high resolution towards the upper end of the distribution. This arrangement allows accurate determination of middle atmosphere cooling rates while preserving the speed of the model (Mlawer *et al.*, 1997). At different atmospheric levels there is a limited range of absorption coefficient values that provide the main contribution to the cooling rate. Therefore when g approaches 1, only a small fraction of the k-distribution will have contributed due to the rapid increase in the function $k(g)$ at the high end of the distribution, which is why a high resolution is required near g=1 (Mlawer *et al.*, 1997). This high resolution in space near g=1 is difficult to achieve while maintaining speed of execution.

(Mlawer *et al.*, 1997) considers three main points when determining the number of spectral bands to use in RRTM:

- Each spectral band can have at most two species with substantial absorption.
- The range of values of the Planck function in each band cannot be extreme.
- The number of bands should be minimal.

An absorbing gas which dominates the absorption within a certain spectral band is termed a 'key species' and it is treated in more detail than other species in the bands that have smaller but still important absorption. These are referred to as 'minor species'. Table 3.1 presents the spectral bands of RRTM in the LW region (Mlawer *et al.*, 1997).

		Species Implemented in RRTM			
		Lower Atmosphere		Middle/Upper Atmosphere	
Band Number	Wavenumber Range, cm_1	Key Species	Minor Species	Key Species	Minor Species
1	10-250	H_2O		H_2O	
2	250-500	H_2O		H_2O	
3	500-630	H_2O, CO_2		H_2O, CO_2	
4	630-700	H_2O, CO_2		13.65, O_3	
5	700-820	H_2O, CO_2	CCl_4	CO_2, O_3	CCl_4
6	820-980	H_2O	CO_2, CFC-11, CFC-12	...	CFC-11, CFC-12
7	980-1080	H_2O, O_3	CO_2	O_3	
8	1080-1180	H_2O	CO_2, CFC-12, CFC-22	O_3	
9	1180-1390	H_2O, CH_4		CH_4	
10	1390-1480	H_2O		H_2O	
11	1480-1800	H_2O		H_2O	
12	1800-2080	H_2O, CO_2		...	
13	2080-2250	H_2O, N_2O		...	
14	2250-2380	CO_2		13.65	
15	2380-2600	CO_2, N_2O		...	
16	2600-3000	H_2O, CH_4		...	

Table 3.1: RRTM Bands (Mlawer *et al.*, 1997)

3.5.1 Accuracy

The LW accuracy of RRTM is 0.6 Wm^{-2} (relative to the LBLRTM) for the net flux in each band at all altitudes with a total error of less than 1.0 Wm^{-2} at any altitude. It recorded an error of 0.07 K d^{-1} for total cooling rate error in the troposphere and lower stratosphere and 0 .75 K d^{-1} in the upper stratosphere (Mlawer *et al.*, 1997).

Results of timing tests for RRTM indicate that computing the fluxes and cooling rates for a 51-layer atmosphere which includes the performance of 256 (16 bands x 16 subintervals) upward and downward radiative transfer calculations and, therefore, the computation of 256 optical depths per layer, takes 0.06 s on a SPARC server 1000. This compares favourably with the other rapid radiative transfer models (Mlawer *et al.*, 1995). A further indication of the computational efficiency of the model is that these radiative transfer operations in RRTM take 1.8 times the amount of time needed to perform 51 x 16 x 16 exponentials. The speed and the accuracy of this model makes it suitable for use in GCMs (Mlawer *et al.*, 1997).

3.6 Full-Spectrum Correlated k-distribution Method (FSCK)

3.6.1 FSCK Method theory

The full-spectrum correlated-k distribution method (FSCK) is similar to the correlated k-distribution method (Li & Modest, 2002). In the FSCK method the absorption coefficients, k, are again sorted into smooth, monotonically increasing cumulative k-distributions, which enables the spectrum to be calculated with fewer calculations. The correlated k-distribution method is limited by the fact that the Planck function must be constant over the spectral range of the absorption coefficients. In the FSCK method, there is no restriction on the Planck function eliminating the need for a constant Planck function across each spectral

region (Pawlak *et al.*, 2004). As a result, in the FSCK approach, spectral bands can now be large, even as big as the full spectrum (Pawlak *et al.*, 2004).

Note that to eliminate the requirement that the Planck function must be constant over the spectral interval being sorted, the k-distribution is redefined using the Planck function as a weighting function. This means that the k-distribution gains temperature dependence through the Planck function (Pawlak *et al.*, 2004). (Stull, 1989) showed that an effective Planck function (the integral of the Planck function over wavenumbers which contribute to absorption in a particular range of g) can be used to replace the Planck function in the radiative transfer equations.

By eliminating the necessity for multiple spectral bands, the total number of calculations can be reduced substantially without losing significant accuracy relative to LBL calculations (Pawlak *et al.*, 2004).

Since FSCK requires quadrature over a single monotonically increasing function and needs about 10 quadrature points, while LBL calculations require about 1 million quadrature points, the FSCK method will greatly speed up the calculations. (Modest & Zhang, 2002) states that FSCK calculations required less than 0.05 seconds to perform defined calculations while the LBL calculations required 25 minutes.

Chapter 4

Method

4.1 Complex Radiative Transfer with Reynolds Decomposition

We can now derive the governing equations of Reynolds Averaged Radiative Transfer. We want to solve the radiative transfer equation (2.18) derived in section 2.3. We will first consider a simplified version of the RTE. We will take this equation but use it in the case where there is emission. The Planck Function B now varies with wavelength. We will also account for radiation travelling in more than one direction. The Diffusivity factor D does not equal zero and will be kept in the derivation. So we can lose the $\hat{\mathbf{\Omega}}$ notation. We begin with equation (2.18) and as we are discounting scattering we can eliminate the third term.

$$\frac{dI}{d\tau} = -I + (1 - \tilde{\omega})B. \tag{4.1}$$

As we are not accounting for scattering, the extinction coefficient is equal to the absorption coefficient. So our single scatter albedo can be written,

$$\tilde{\omega} = \frac{\beta_s}{\beta_a}. \tag{4.2}$$

We can then times through by the optical depth $d\tau{=}\beta_a ds$,

$$dI = -I\beta_a ds + (1 - \frac{\beta_s}{\beta_a})B\beta_a ds. \tag{4.3}$$

As scattering is not included, the term involving β_s disappears and we are left with Schwarzschild's Equation

$$dI = \beta_a(B - I)ds. \tag{4.4}$$

We must now times by the diffusivity factor to account for radiation travelling in multiple directions. We shall denote the irradiance I as the flux F, and change the space step ds into dz to represent a vertical path through the atmosphere.

$$dF = -D\beta_a\,(F - B)\,dz. \tag{4.5}$$

Reynolds Decomposition is then used to derive the Reynolds Averaged Radiative Transfer Equations.

Equation (4.5) shows the basic Radiative Transfer Equation for Infra Red wave lengths in the absence of scattering. The diffusivity factor accounts for the fact radiation does not just travel upwards, it also travels at an angle to the vertical. So the mean path through a layer of thickness dz is no longer length D. Typically D is assumed to be 1.66. β is the Extinction/absorption Coefficient, which are equivalent in the absence opf scattering (m^{-1}), F is the radiative flux (Wm^{-2}) or ($\mathrm{Wm}^{-2}(\mathrm{cm}^{-1})^{-1}$) or flux per unit wave number. B is the Planck function (Wm^{-2}) or ($\mathrm{Wm}^{-2}(\mathrm{cm}^{-1})^{-1}$) and dF is the change in upward or downward flux over a short distance dz.

β varies rapidly with wavelength. B and F also change with wavelength. We will now use the idea of Reynolds Averaging to account for this variability. We can decompose the fluctuating components of (4.5), β, B and F into a time averaged component represented by $\overline{\beta}$, $\overline{B}$ and $\overline{F}$ and the deviation from that average represented by β', B' and F'. By definition $\overline{F'} = 0$

$$dF = d\overline{F} + dF' \tag{4.6a}$$
$$\beta = \overline{\beta} + \beta' \tag{4.6b}$$
$$F = \overline{F} + F' \tag{4.6c}$$
$$B = \overline{B} + B' \tag{4.6d}$$

We begin by taking (4.5) and substituting into it the Reynolds decomposed versions of the variables found in (4.6):

$$\left(d\overline{F} + dF'\right) = -D\left(\overline{\beta} + \beta'\right)\left(\overline{F} + F' - \overline{B} - B'\right)dz. \tag{4.7}$$

We can then multiply out the brackets:

$$\left(d\overline{F} + dF'\right) = -D\left(\overline{\beta}\,\overline{F} + \overline{\beta}F' - \overline{\beta}\,\overline{B} - \overline{\beta}B' + \beta'\overline{F} + \beta'F' - \beta'\overline{B} - \beta'B'\right)dz. \tag{4.8}$$

We now average over the whole spectrum, using rules 4, 5 and 6 from section 2.5, so any term with only one prime will cancel leaving

$$d\overline{F} = -D\left(\overline{\beta}\,\overline{F} - \overline{\beta}\,\overline{B} + \overline{\beta'F'} - \overline{\beta'B'}\right)dz \tag{4.9}$$

This equation contains a covariance term which in principle we know $\overline{\beta'B'}$, the covariance of the known spectral variation of the Planck Function with the known variation of the absorption coefficient.

the equation also contains a term we do not know $\overline{\beta'F'}$. We can derive an expression for it by subtracting equation (4.9) from (4.8)

$$\begin{aligned}\left(d\overline{F} + dF'\right) - d\overline{F} = \; &- \; D\left(\overline{\beta}\,\overline{F} + \overline{\beta}F' - \overline{\beta}\,\overline{B} - \overline{\beta}B' + \beta'\overline{F} + \beta'F' - \beta'\overline{B} - \beta'B'\right)dz \\ &+ \; D\left(\overline{\beta}\,\overline{F} - \overline{\beta}\,\overline{B} + \overline{\beta'F'} - \overline{\beta'B'}\right)dz.\end{aligned} \tag{4.10}$$

$$dF' = -D\left(+\overline{\beta}F' - \overline{\beta}B' + \beta'\overline{F} + \beta'F' - \beta'\overline{B} - \beta'B' - \overline{\beta'F'} + \overline{\beta'B'}\right)dz. \quad (4.11)$$

We want an equaiton for $d\overline{\beta'F'}$ to predict $\overline{\beta'F'}$. Using the chain rule we can expand $d\overline{\beta'F'}$

$$d\overline{\beta'F'} = \overline{\beta'dF'} + \overline{F'd\beta'}. \quad (4.12)$$

We are treating the extinction coefficient as constant along a path so $d\beta' = 0$

$$d\overline{\beta'F'} = \overline{\beta'dF'}. \quad (4.13)$$

We can now times (4.11) by β' and take the average over the spectrum.

$$\overline{\beta'dF'} = d\overline{\beta'F'} = -D\left(\overline{\beta}\,\overline{\beta'F'} - \overline{\beta}\,\overline{\beta'B'} + \overline{\beta'^2}\,\overline{F} - \overline{\beta'^2}\,\overline{B} - \overline{\beta'^2F'} - \overline{\beta'^2B'}\right)dz. \quad (4.14)$$

The last two terms in (4.11) disappear when the average is taken and we obtain (4.14) which again contains an unknown, this time of a higher order $\overline{\beta'^2F'}$

We can follow the same procedure again to obtain an equation for the new unknown.

$$d\overline{\beta'^2F'} = \overline{\beta'^2dF'} = -D\left(\overline{\beta'^3\,F'} - \overline{\beta'^3}\,\overline{B} + \overline{\beta}\,\overline{\beta'^2F'} - \overline{\beta}\,\overline{\beta'^2B'} + \overline{\beta'^3F'} - \overline{\beta'^3B'}\right)dz. \quad (4.15)$$

Now we again have another unknown this time of higher order $\overline{\beta'^3B'}$ again this is a closure problem. We could keep on deriving equations for the unknowns, however, each time we derive a new equation, it will have a new unknown of one higher order than that of the term we are trying to derive. This is known as the closure problem Stull (1989). We overcome this problem, by parameterizing the unknown term at a certain stage where we require a certain accuracy.

So up to third order accuracy we can define F by these three equations

$$\frac{d\overline{F}}{dz} = -D(\overline{\beta}\,\overline{F} - \overline{\beta}\,\overline{B} + \overline{\beta' F'} + \overline{\beta' B'}+) \tag{4.16a}$$
$$\frac{d\overline{\beta' F'}}{dz} = -D(\overline{\beta'^2}\,\overline{F} - \overline{\beta'^2}\,\overline{B} + \overline{\beta}\,\overline{\beta' F'} + \overline{\beta'^2 F'} - \overline{\beta}\,\overline{\beta' B'} - \overline{\beta'^2 B'}) \tag{4.16b}$$
$$\frac{d\overline{\beta'^2 F'}}{dz} = -D(\overline{\beta'^3}\,\overline{F} - \overline{\beta'^3}\,\overline{B} + \overline{\beta}\,\overline{\beta'^3 F'} + \overline{\beta'^3 F'} - \overline{\beta}\,\overline{\beta'^2 B'} - \overline{\beta'^3 B'}) \tag{4.16c}$$

If we set: $F = \overline{F}$, $G = \overline{\beta' F'}$, $H = \overline{\beta'^2 F'}$, $I = \overline{\beta'^3 F'}$, $J = \overline{\beta' B'}$, $K = \overline{\beta'^2 B'}$ and $L = \overline{\beta'^3 B'}$ we obtain:

$$\frac{dF}{dz} = -D(\overline{\beta}\,F - \overline{\beta}\,\overline{B} + G + J) \tag{4.17a}$$
$$\frac{dG}{dz} = -D(\overline{\beta'^2}\,F - \overline{\beta'^2}\,\overline{B} + \overline{\beta}\,G + H - \overline{\beta}\,J - K) \tag{4.17b}$$
$$\frac{dH}{dz} = -D(\overline{\beta'^3}\,F - \overline{\beta'^3}\,\overline{B} + \overline{\beta}\,H + I - \overline{\beta}\,K - L) \tag{4.17c}$$

It is clear that 4.17 is a system of coupled, linear diffrential equations and can be solved by :

$$\begin{pmatrix} \frac{dF}{dz} \\ \frac{dG}{dz} \\ \frac{dH}{dz} \end{pmatrix} = -D \begin{pmatrix} \overline{\beta} & 1 & 0 & 0 & 1 & 0 & 0 \\ \overline{\beta'^2} & \overline{\beta} & 1 & 0 & -\overline{\beta} & -1 & 0 \\ \overline{\beta'^3} & 0 & \overline{\beta} & 1 & 0 & -\overline{\beta} & -1 \end{pmatrix} \begin{pmatrix} F \\ \vdots \\ L \end{pmatrix} + D\overline{B} \begin{pmatrix} \overline{\beta} \\ \overline{\beta'^2} \\ \overline{\beta'^3} \end{pmatrix}$$

We can write the inhomogeneous linear a system as:

$$\frac{d\mathbf{x}}{dz} = \mathbf{A}\mathbf{x} + \mathbf{c} \tag{4.18}$$

4.2 Simple Radiative Transfer with Reynolds Decomposition

We will simplify the above example even further. In the case where the Planck Function B equals zero (no emission) and the Diffusivity Factor D equals one (Radiation travels in only one direction). Equation (4.5) can now be written,

$$dF = -\beta_a F dz, \tag{4.19}$$

where β_a varies rapidly with wavelength and F also changes with wavelength. We can follow the same process as in the example above were we use Reynolds Averaging to account for this variability.

Substituting the three Reynolds Decomposed components from (4.6) into (4.19), averaging over the spectrum of wavelengths being considered as carried out above we obtain, where terms with one prime have been cancelled:

$$d\overline{F} = -\left(\overline{\beta}\,\overline{F} + \overline{\beta' F'}\right) dz. \tag{4.20}$$

$d\overline{F}$... $\overline{\beta}\,\overline{F}$ represents the... $\overline{\beta' F'}$ is an unknown

As before we can form an equation to estimate this term form what we already know by subtracting $d\overline{F}$ from $(d\overline{F} + dF')$ and using the chain rule (4.12) treating the extinction coefficient as constant along a path so $d\beta' = 0$ we can now times (**??**) by β' and take the average over the spectrum.

$$d\overline{\beta' F'} = -\left(\overline{\beta'^2}\,\overline{F} + \overline{\beta}\,\overline{\beta' F'} + \overline{\beta'^2 F'}\right) dz. \tag{4.21}$$

All terms are terms we have calculated already or things we can calculate except $\overline{\beta'^2 F'}$ is an unknown

We can now carry out the same procedure to form an equation which approximates the above unknown. This will however lead to a further unknown in the

new approximation, this time of order 3.

$$d\overline{\beta'^2 F'} = -\left(\overline{\beta'^3}\,\overline{F} + \overline{\beta}\,\overline{\beta'^2 F'} + +\overline{\beta'^3 F'}\right) dz \tag{4.22}$$

Now $\overline{\beta'^3 F'}$ is an unknown.

Up to third order accuracy we can define F by these three equations:

$$\frac{d\overline{F}}{dz} = -\overline{\beta}\,\overline{F} - \overline{\beta' F'} \tag{4.23a}$$
$$\frac{d\overline{\beta' F'}}{dz} = -\overline{\beta'^2}\,\overline{F} - \overline{\beta}\,\overline{\beta' F'} - \overline{\beta'^2 F'} \tag{4.23b}$$
$$\frac{d\overline{\beta'^2 F'}}{dz} = -\overline{\beta'^3}\,\overline{F} - \overline{\beta}\,\overline{\beta'^2 F'} - \overline{\beta'^3 F'} \tag{4.23c}$$

If we set $F = \overline{F}$, $G = \overline{\beta' F'}$, $H = \overline{\beta'^2 F'}$ and $I = \overline{\beta'^3 F'}$ we obtain:

$$\frac{dF}{dz} = -\overline{\beta}\,F - G \tag{4.24a}$$
$$\frac{dG}{dz} = -\overline{\beta'^2}\,F - \overline{\beta}\,G - H \tag{4.24b}$$
$$\frac{dH}{dz} = -\overline{\beta'^3}\,F - \overline{\beta}\,H - I \tag{4.24c}$$

It is clear that 4.24 is a system of coupled, linear, homogeneous differential equations and can be solved by:

$$\begin{pmatrix} \frac{dF}{dz} \\ \frac{dG}{dz} \\ \frac{dH}{dz} \end{pmatrix} = \begin{pmatrix} -\overline{\beta} & -1 & 0 & 0 \\ -\overline{\beta'^2} & -\overline{\beta} & -1 & 0 \\ -\overline{\beta'^3} & 0 & -\overline{\beta} & -1 \end{pmatrix} \begin{pmatrix} F \\ G \\ H \\ I \end{pmatrix}$$

We can write the homogeneous linear a system as:

$$\frac{d\mathbf{x}}{dz} = \mathbf{A}\mathbf{x}. \tag{4.25}$$

Again we have a closure problem as described in the previous section. The unknown must be parameterized in order to solve the system, defining a closure approximation. The closure problem is defined when the total statistical description of the system requires an infinite set of equations (Liou, 1992).

We can parameterize the term $\overline{\beta'^2 F'}$ and solve the first two equations in (4.23), this would be a second order closure problem. Or we can could parameterize the term $\overline{\beta'^3 F'}$ and solve the three equations, this would be third order closure.

4.3 Model Description

The computer program was written to solve the problem in section 4.2. The transmittance is calculated along a homogeneous vertical path through the atmosphere where all radiation is travelling in the same direction (D=1) and there is no emission. The path is divided into a number of layers, nz, each of length, dz. The absorption spectrum is the same at each layer, z (4.1).

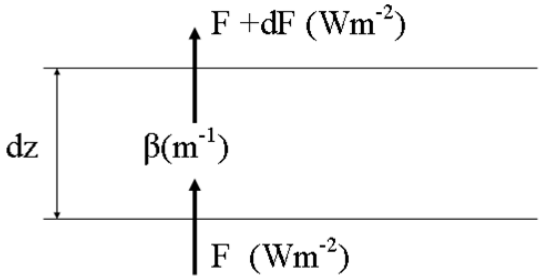

Figure 4.1: Discretization of atmosphere into nz layers of length dz and the change in flux across that layer due only to absorption

We form the absorption spectrum by randomly generating each coefficient, x, to conform to either a normal distribution or a Gaussian distribution. Due to the absence of scattering, the extinction coefficient is equivalent to the absorption coefficient. The absorption coefficient is then obtained by taking the exponential

of x, so a normal distribution of x will lead to a log normal distribution of absorption coefficient. It is possible to think of the number of different absorption coefficients as the number of different wavelengths being considered, as the extinction is different at each wavelength. Absorption coefficient is constant with range so we can define the optical depth as:

$$d\tau = \beta_a z. \tag{4.26}$$

This leads onto the transmission at each layer, z and at each wavelength, which is the solution to equation(2.9):

$$\text{Trans} = \exp(-\beta_a z). \tag{4.27}$$

The true transmission is equivalent to the LBL calculations and is the average of the transmission at each wavelength. The exact second order system is calculated by solving the first two equations in (4.23) and parameterizing the unknown $\overline{\beta'^2 F'}$ by setting it equal to the standard deviation of the known term $\beta'\overline{\beta' F'}$.

The second and third order numerical solutions of the transmission is calculated using a forward Euler method looping over the range, z. The third order paramteterization of $\overline{\beta'^3} F'$ is to set this term equal to $5\times\overline{\beta'^2 F'}\times\sigma\beta'$. We can therefore take (4.23)

The model is then run with real atmospheric data for absorption coefficient spectrums read into the program from an external file. The spectrum is shown in figure (4.2) and includes the extinction due to the gases: CO_2, H_2O and O_3.

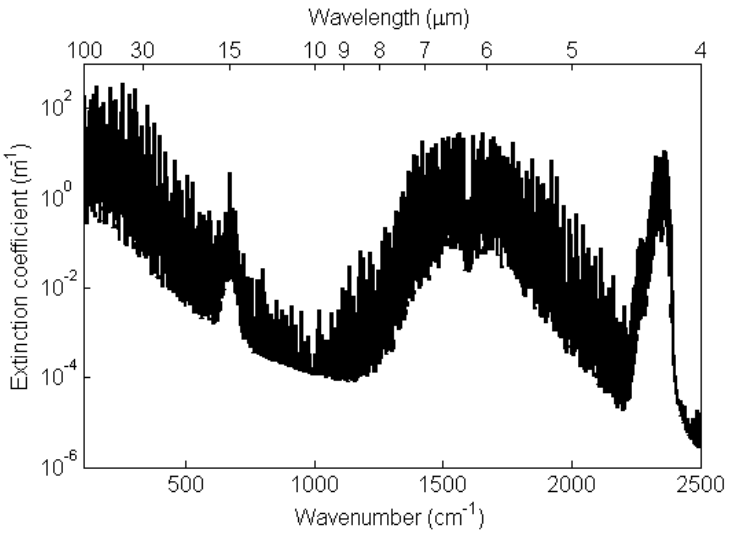

Figure 4.2: Extinction coefficient spectrum due to CO_2, H_2O and O_3 in the IR region

The extinction coefficient is measured in m^{-1} as it is a measure of the molecular absorption cross-section, per m^3 of air.

The external file also includes data for the Planck function over the wavelength spectrum shown in figure (4.3).

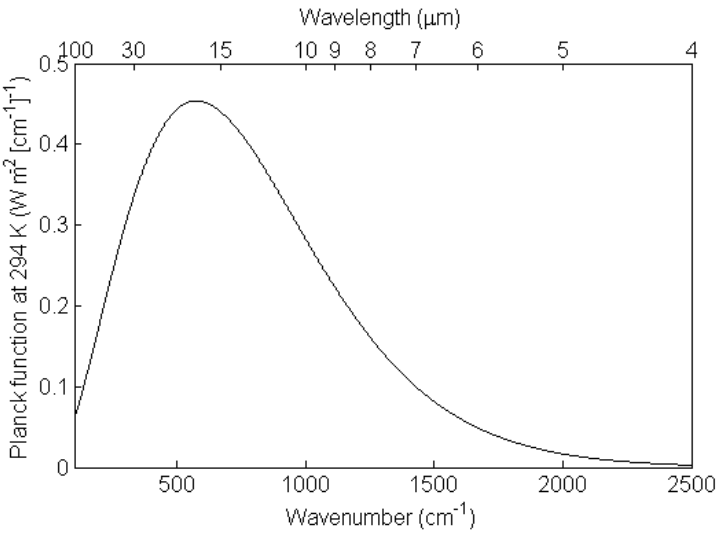

Figure 4.3: Varitation of Planck Function with wavelength and wavenumber in over IR region

Chapter 5

Results

5.1 Basic Model

5.1.1 Normal Distribution

Figure (5.1) shows the transmittance along a homogeneous path through the atmosphere. The thick black line represents the true transmittance and is equivalent to the LBL calculations. These graphs were obtained using 5000 points in z and a space step of, dz = 20.

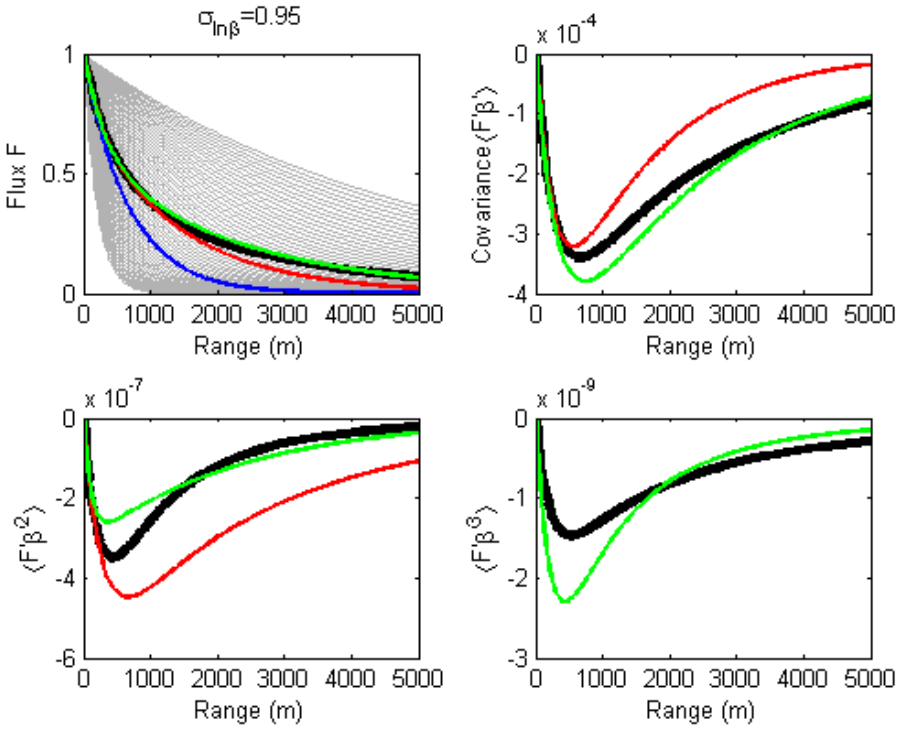

Figure 5.1: Blue = numerical first order transmittance, red = second order numerical transmittance, green = numerical third order transmittance. Normal distribution, σ=0.95.

The blue line represents the numerical first order radiative transfer when the fluctuating terms are averaged across the whole spectrum. The scaling factor is 0.357 which determines the spread of the absorption coefficients, this results in a standard deviation, σ, of 0.95. The red line is the second order numerical transmittance and the green line is the numerical third order transmittance. The many grey lines represent the raw transmissions of each absorption coefficient. There are 61 absorption coefficients in the spectrum. It is therefore clear form figure 5.1 that the absorption coefficient spectrum is normally distributed represented by figure 5.2.

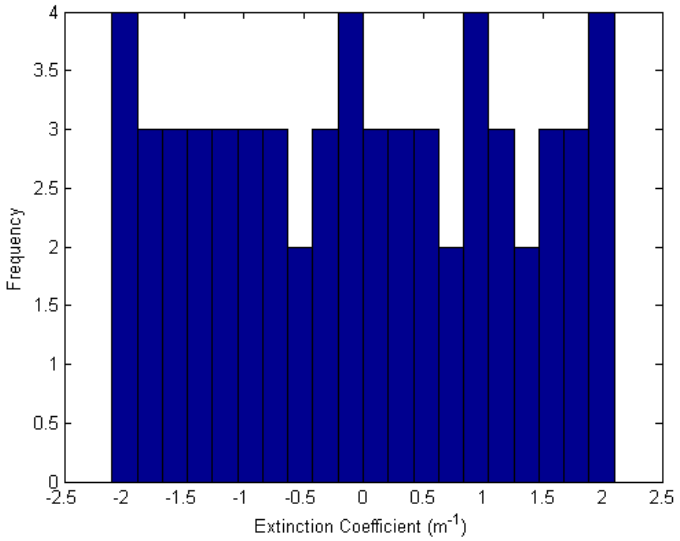

Figure 5.2: Histogram of extinction coefficients, normally distributed.

Figure 5.3 represents the transmission with again, a normal distribution of absorption coefficients, however, this time the standard deviation of the absorption coefficients is greater σ=1.78. The scaling factor is equal to one.

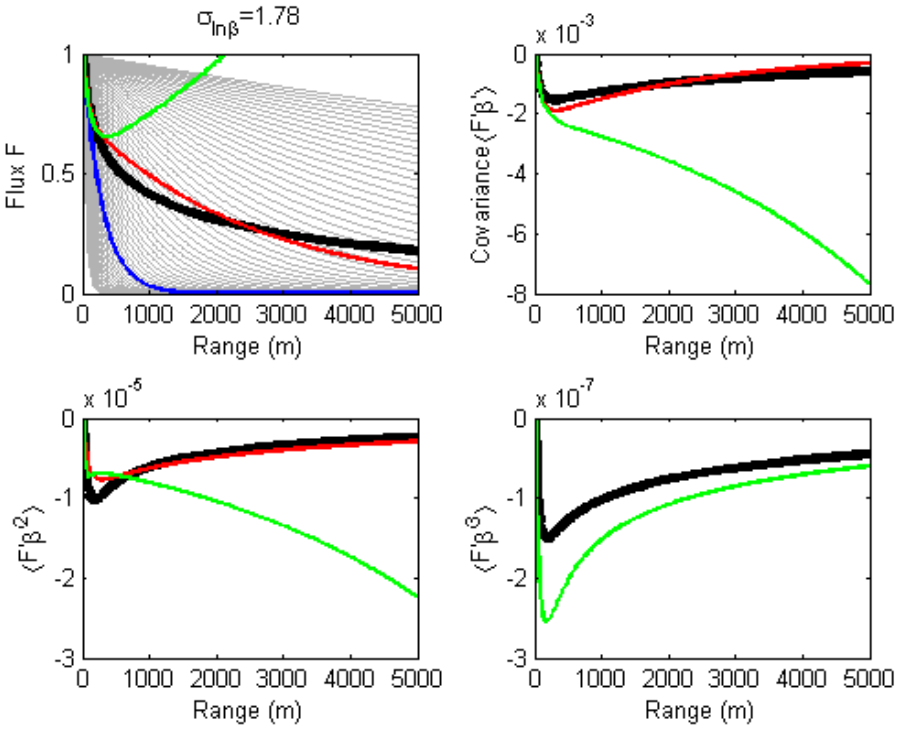

Figure 5.3: Blue = numerical first order transmittance, red = second order numerical transmittance, green = numerical third order transmittance. Normal distribution, σ=1.78.

Figure 5.4 represents the same again, however this time the standard deviation is even greater, σ=2.13 with a scaling factor of 1.2.

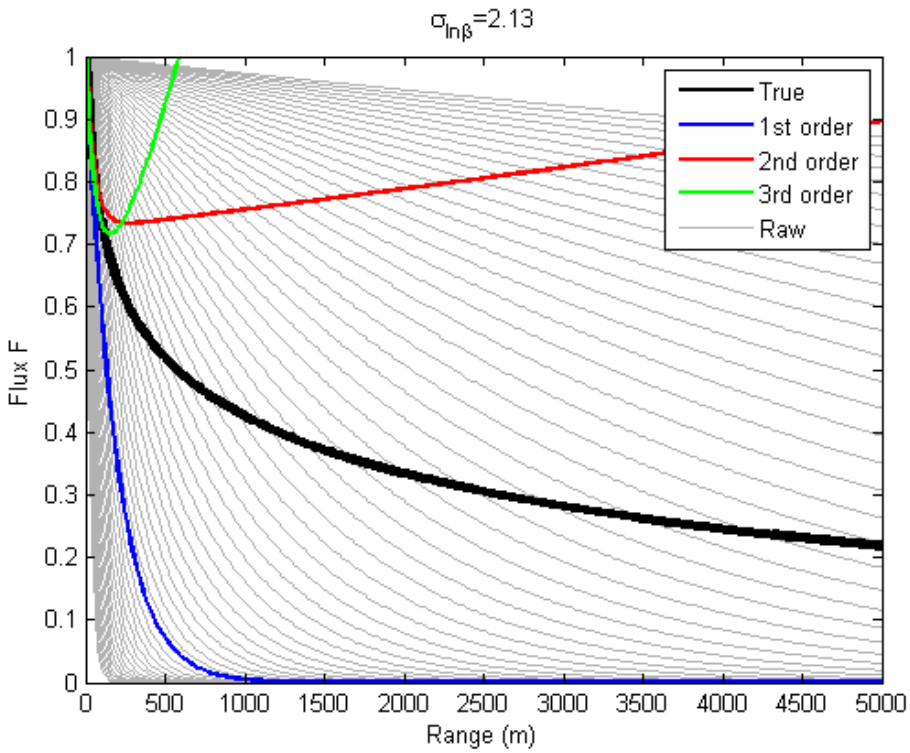

Figure 5.4: Blue = numerical first order transmittance, red = second order numerical transmittance, green = numerical third order transmittance. Normal distribution, σ=2.13.

The variation in covariance has not been plotted as the third order (green) covariance approximation quickly falls away from the true solution for the covariance term.

5.1.2 Gaussian

We shall now look at the same program, however this time, the randomly generated absorption coefficients will adhere to a Gaussian distribution. Figure 5.5 has the same standard deviation (0.95) as figure 5.1.

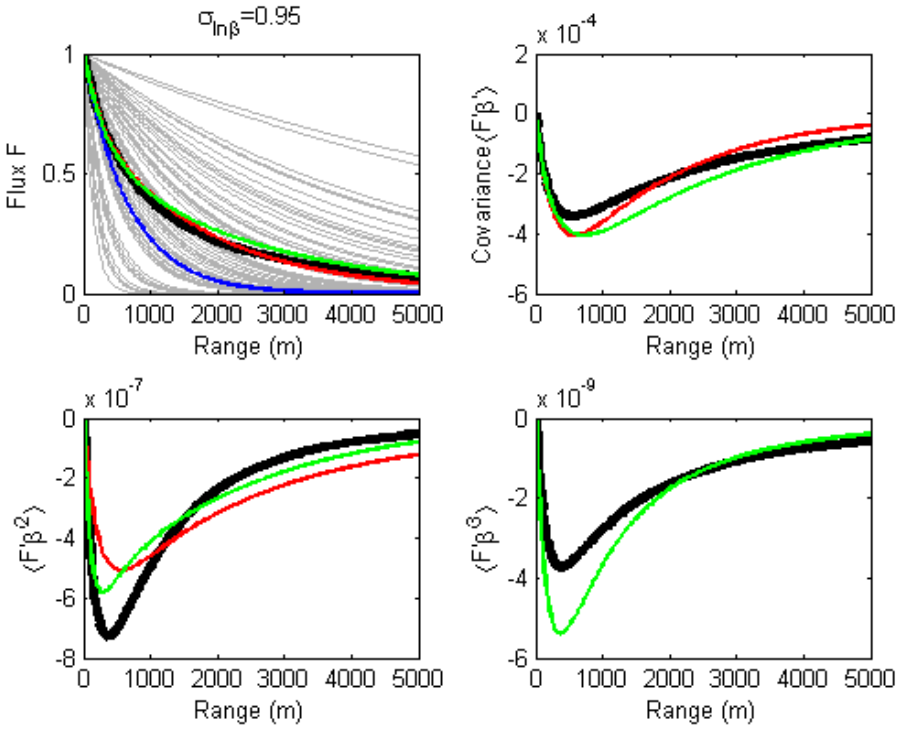

Figure 5.5: Blue = numerical first order transmittance, red = second order numerical transmittance, green = numerical third order transmittance. Gaussian distribution, σ=0.95.

Figure 5.5 has a scaling factor of one to achieve the standard deviation σ = 0.95 and also has 61 absorption coefficients in the spectrum. It is clear from the raw transmission for each individual absorption coefficient (faint grey lines) that the distribution is Gaussian, represented in figure 5.6.

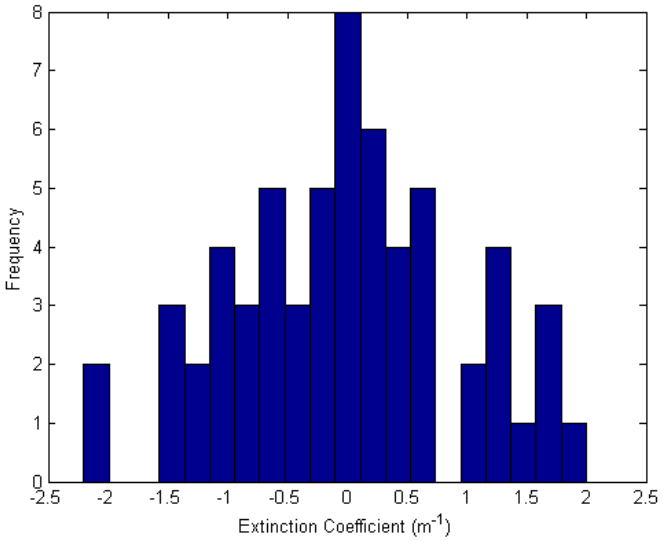

Figure 5.6: Histogram of extinction coefficients, Gaussian distributed.

It appears that for the same standard deviation in a normal distribution, figure 5.1 and a Gaussian distribution, figure 5.5, the Gaussian distribution is more accurate at approximating the transmittance along the path. As the distribution is Gaussian however, each time the model is run, the distribution changes. Figure 5.7 has the same standard deviation, $\sigma = 0.95$, as figure 5.5, yet has produced different approximations for each of the first, second and third order transmissions.

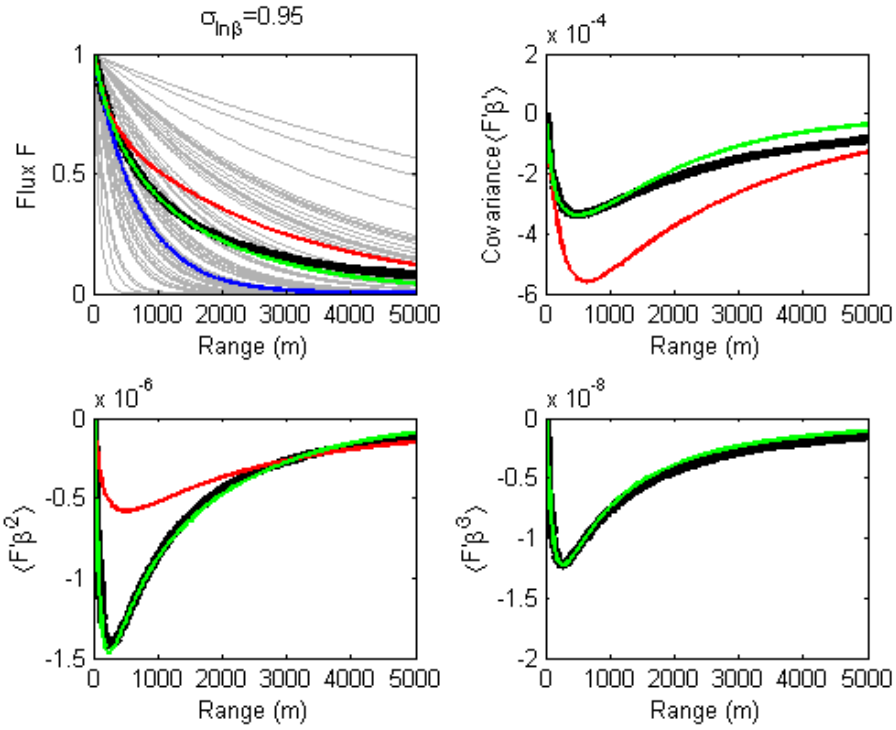

Figure 5.7: Blue = numerical first order transmittance, red = second order numerical transmittance, green = numerical third order transmittance. Gaussian distribution, σ=0.95.

Figure 5.8 has a scaling factor of 1.89 to achieve the standard deviation the same as figure 5.3 yet the second order approximation has blown up very quickly and the third order transmission drops quickly to zero.

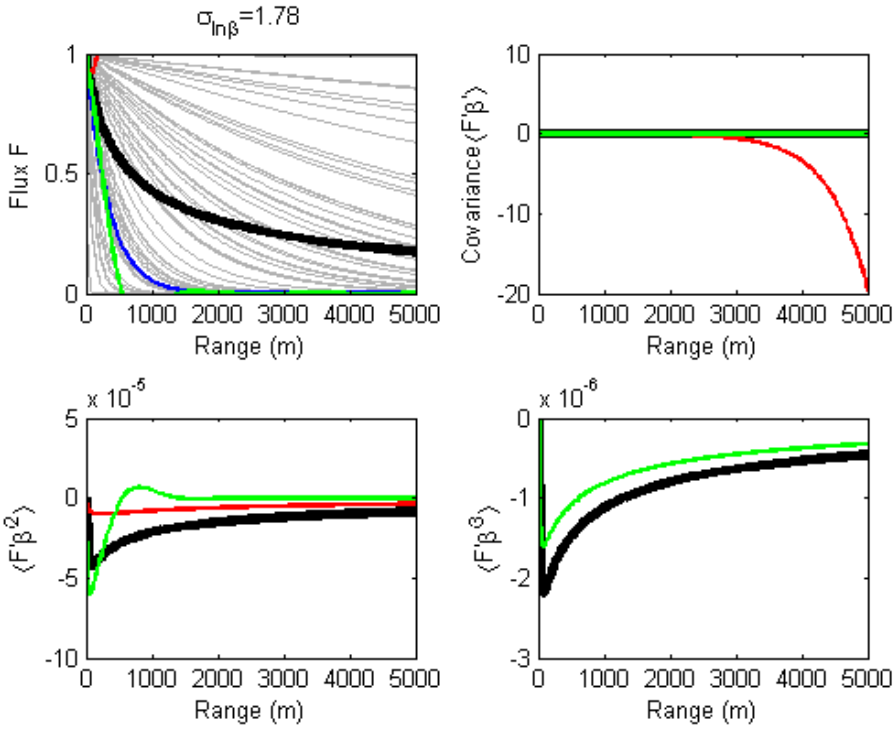

Figure 5.8: Blue = numerical first order transmittance, red = second order numerical transmittance, green = numerical third order transmittance. Gaussian distribution, σ=1.78.

5.2 Simple two band model

5.2.1 Normal

A simple two band model was created by finding the mean extinction coefficient and putting all the extinction coefficients smaller than the median into one bin and then putting all the extinction coefficients greater or equal to the median into a second bin. Figure 5.9 has a normally distributed absorption spectrum and has the same standard deviation as the normal distribution figure 5.1.

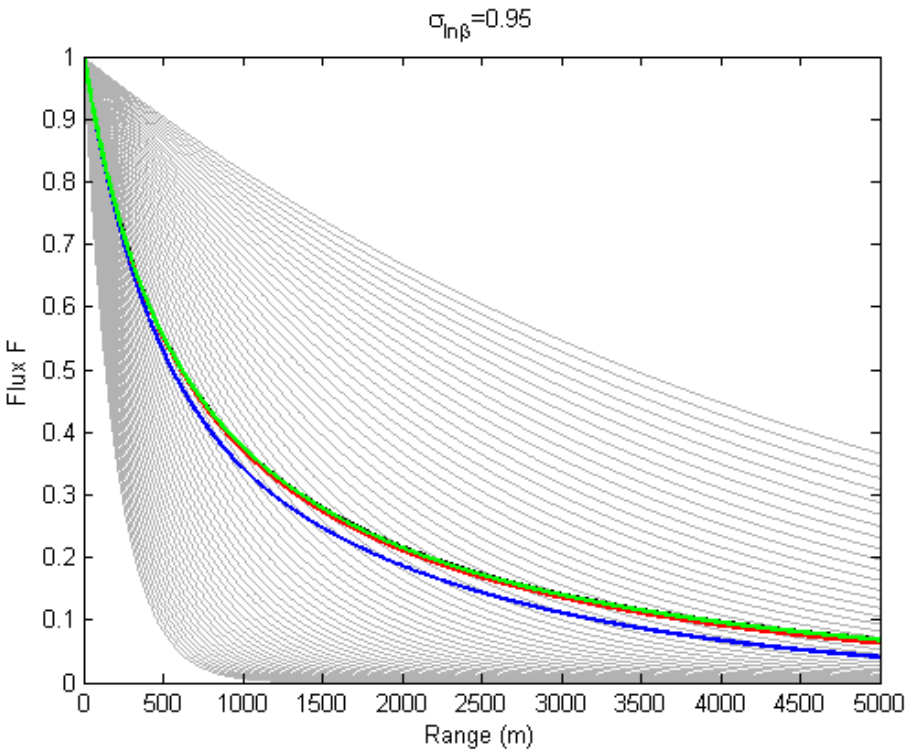

Figure 5.9: Two band model. Blue = numerical first order transmittance, red = second order numerical transmittance, green = numerical third order transmittance. Normal distribution, σ=0.95.

5.2.2 Gaussian

Figure 5.10 has a Gaussian distribution of absorption coefficients and has the same standard deviation as the Gaussian distributed figure 5.5.

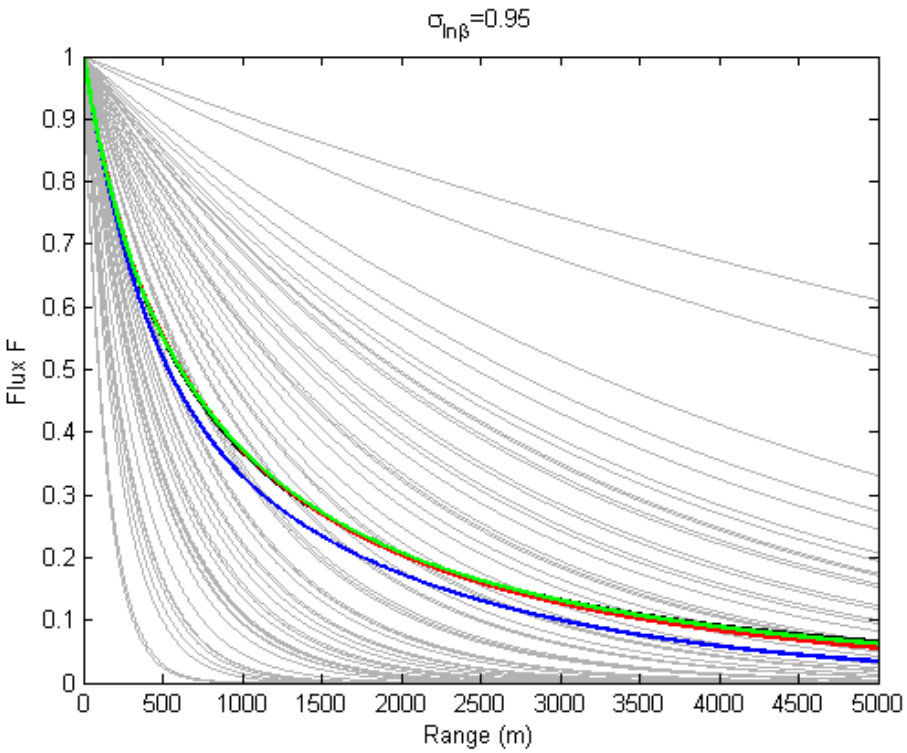

Figure 5.10: Two band model. Blue = numerical first order transmittance, red = second order numerical transmittance, green = numerical third order transmittance. Gaussian distribution, σ=0.95.

5.3 Equal weight band model

In order for better accuracy we can look to split the spectrum up into more bands. However we need to find a new way to define each band. In the following section the results are obtained from the model where each band in the spectrum has the same number of absorption coefficients within them. So each band has an equal weight and an equal fraction of the spectrum.

5.3.1 Atmospheric data

In the absorption coefficient spectrum, there are 9610 values plotted in figure 4.2. Figure 5.11 was produced sampling every single absorption coefficient. The model takes a while to run, sampling 9610 points. Figure 5.11 shows the route mean squared (RMS) accuracy of the transmission of the first second and third order numerical approximations compared to the true transmission as the number of bands in the model is increased.

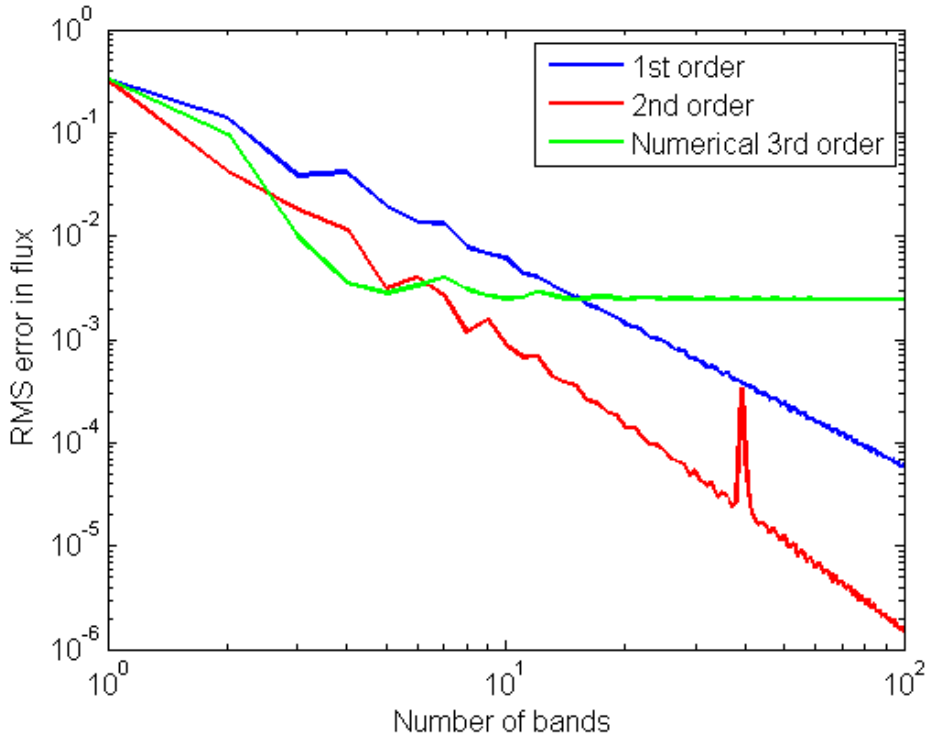

Figure 5.11: Equally weighted bands. Blue = numerical first order transmittance RMS error, red = second order numerical transmittance RMS error, green = numerical third order transmittance RMS error, for atmospheric data.

We can however sample a smaller number of extinction coefficients such as every 30 shown in figure 5.12.

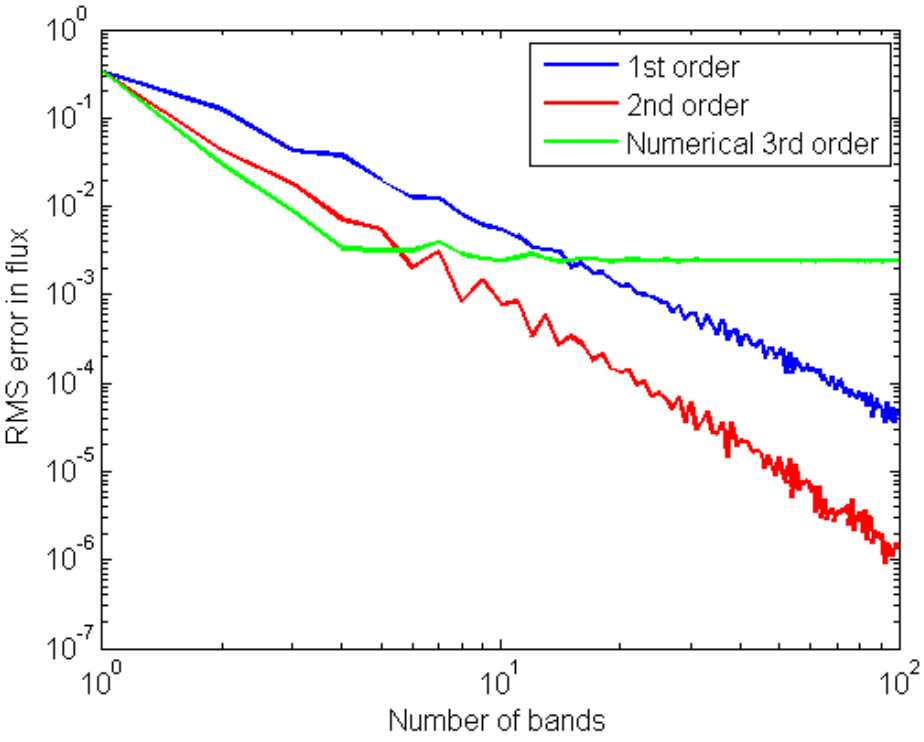

Figure 5.12: Equally weighted bands. Blue = numerical first order transmittance RMS error, red = second order numerical transmittance RMS error, green = numerical third order transmittance RMS error, for atmospheric data.

5.4 Weighted average band model

This provides an alternative way of defining the bands in the spectrum. This time, instead of having an equal number of absorption coefficients within each bands, the number will vary. Each band will take an equal fraction of the dynamic range, meaning each band will cover a certain order of magnitude. As each band has a differing number of absorption coefficients within it, we therefore need to calculate a weighted average of the bands in order to calculate the total flux. So each band will be weighed by the number of extinction coefficients.

5.4.1 Atmospheric data

Figure 5.13 was produced sampling every single absorption coefficient. Figure 5.13 shows the route mean squared (RMS) accuracy of the transmission of the first, second and third order numerical approximations compared to the true transmission as the number of bands in the model is increased.

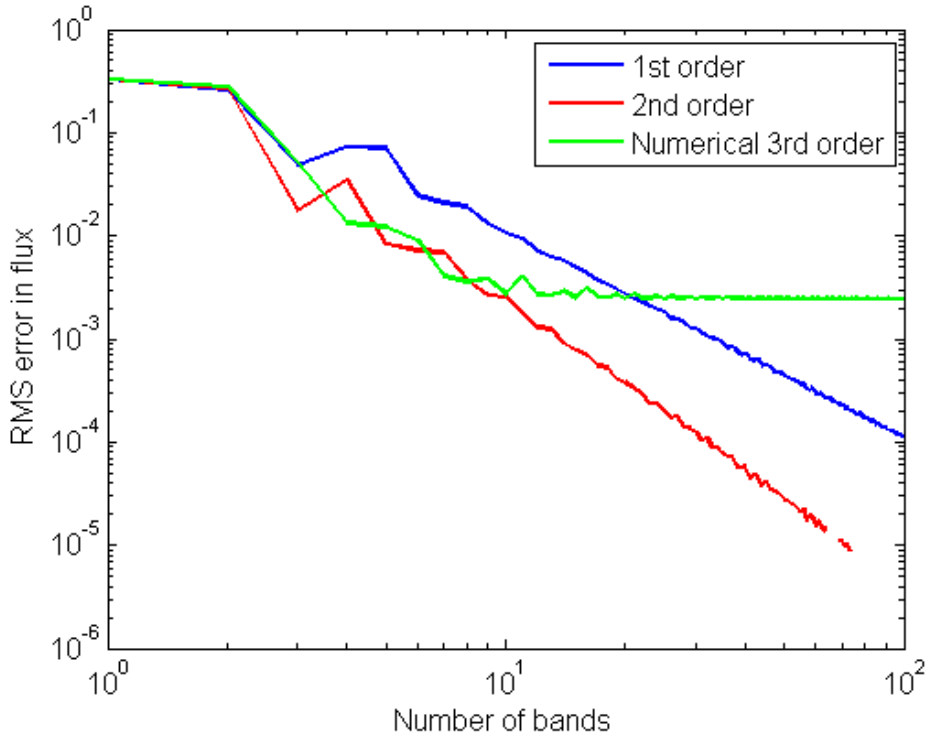

Figure 5.13: Weighted bands. Blue = numerical first order transmittance RMS error, red = second order numerical transmittance RMS error, green = numerical third order transmittance RMS error, for atmospheric data.

Figure 5.14 was produced sampling every 20th absorption coefficient. The model samples 480 points. Already the first order approximation is beginning to blow up. So with this technique we have to carry out a finer sample of absorption coefficient.

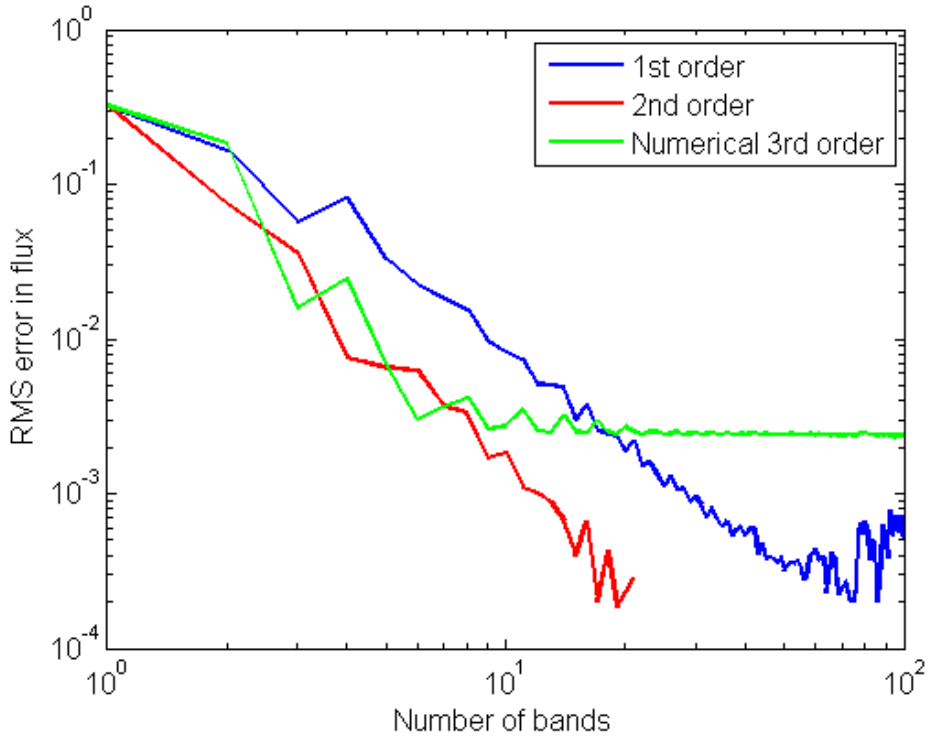

Figure 5.14: Weighted bands. Blue = numerical first order transmittance RMS error, red = second order numerical transmittance RMS error, green = numerical third order transmittance RMS error, for atmospheric data sampling every 20^{th} coefficient.

Figure 5.15 shows a histogram for the range of absorption coefficients in the atmospheric data set. It is clear that there is a large number of small coefficients and a very sparse number of larger coefficients. Due to the sparseness of the data at the higher end of the range, it is necessary to determine the weighted band intervals in log space, otherwise, there will be some bands which will have no absorption coefficients within them.

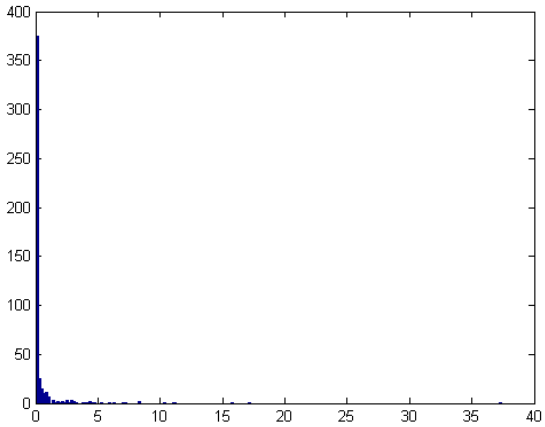

Figure 5.15: Histogram of atmospheric data extinction coefficients.

Chapter 6

Discussion

For a normal distribution of absorption coefficients and a standard deviation of, $\sigma = 0.95$, figure 5.1, it is clear that the third order approximation gives the most accurate transmission through the path, dz. With this model the amount of absorption coefficients does not affect the accuracy. If the normal distribution is widened, the standard deviation increased, then the greater chance of the approximation becoming unstable. If the scaling factor is reduced, there approximation becomes more accurate. With a high standard deviation of 1.78 in figure 5.3 the third order scheme has become unstable and has blown up. With the standard deviation even higher at 2.13, figure 5.4, the second order approximation also becomes unstable. As the standard deviation increases, the numerical scheme is less able to cope with the wider range in absorption coefficients. The smaller the range in extinction coefficient the more accurate the approximation.

The more extreme a single value of absorption coefficient within the spectrum, either negative or positive, then the less accurate the approximations become. Compare figure 5.5, standard deviation of 0.95 with figure 5.8, standard deviation of 1.78. With the higher spread of absorption coefficient, the second order scheme has blown up very quickly and in third order scheme, the transmission dropped quickly to zero. So the more the Gaussian distribution is spread across the wavelengths, the more unstable the numerical approximations become.

Each time the model is run with the Gaussian distribution, as the numbers

are generate randomly, a different spectrum is produced each time. This can lead to a very different distribution with the same standard deviation, dramatically affecting the ability to produce accurate results. This is shown by comparing figure 5.7 with figure 5.5, which have the same standard deviation, 0.95, yet they have both produced different approximations for each of the first, second and third order transmissions.

In section 5.2, it is clear that by simply splitting the spectrum into two bands, the accuracy of all the three different schemes are better at approximating the true transmission. Both the normal and Gaussian distributions have improved their accuracy compared to performing the calculation across the whole spectrum.

Figure 5.9 samples all 9610 absorption coefficients in the atmospheric data file and represents the accuracy of the numerical schemes compared to the true transmission when the number of bands (each with the same number of absorption coefficients) is increased from one to 100. An accuracy of 10^{-6} Wm^{-2} is achieved for 100 bands. This is an acceptable error for the scheme.

It is not essential to sample the absorption coefficient at every value. Relatively good accuracy is achievable by sampling every 10 or 20, figure 5.12. In sampling the absorption spectrum more sparsely we can reduce the time taken to compute the transmission. The numerical third order approximation is the quickest to increase in accuracy as the number of bands are increased, however at around 15 bands, the accuracy levels off, the reasons why need to be investigated. The numerical second order approximation is the most accurate reaching a RMS error of 10^{-6} Wm^{-2} by 100 bands. The first order approximation reaches an RMS error of 10^{-4} Wm^{-2} by 100 bands.

We would expect the band model in section 5.4, which has a equal fraction of the dynamic range to perform better in terms of accuracy, as a relatively larger number of lesser important (smaller absorption coefficients) are treated all together than when each band has an equal number of absorption coefficients. This means that the more important, larger absorption coefficients are treated across more bands so are considered in greater detail than in the equally weighted band model. This would appear to be disputed however as figures 5.11 and 5.12

are producing results to a greater accuracy than the equally weighted band model, figures 5.13 and 5.14.

Is is clear that the models discussed have difficulty in handling a large range in extinction coefficient, this is why bands are so important and have been used throughout the development of radiative transfer models. They enable a smaller range of absorption coefficients to be considered within each band and therefore give a better approximation of the transmission, however every time a new band is added to the model, more computational power is required so it would be better if it were possible to treat the whole spectrum as one band as is done in the FSCK method, using only one radiative transfer calculation and averaging the absorption coefficient across the whole spectrum.

Chapter 7

Conclusions

The next step in the development and testing of a Reynolds averaged radiative transfer model would be to include radiation travelling in different directions, D=1.66 and to also include emission along the path, therefore having to include the planck function. This would involve solving the systems of equations in (4.17). Then we would like to account for scattering. We would also like to account for an inhomogeneous path, where pressure and temperature change, i.e. vertically through the atmosphere, so the absorption spectrums of the gases will change due to pressure broadening.

The next step might be to develop the maths for application to shortwave atmospheric radiative transfer and ultimately to develop a radiative transfer module that may be used in operational numerical weather prediction or GCMs. Comparisons between the newly developed method and current models would be required to determine the relative accuracy of the model. The use of Reynolds decomposition within the radiative transfer equations has the potential for improving the computational requirements of the radiative transfer code relative to traditional correlated k-distribution methods.

References

Clough, S.A., Shephard, M.W., Mlawer, E.J., Delamere, J.S., Iacono, M.J., Cady-Pereira, K., Boukabara, S. & Brown, P.D. (2005). Atmospheric radiative transfer modeling: a summary of the AER codes. *Journal of Quantitative Spectroscopy Radiative Transfer*, **91**, 233244.

Coelhoa, P.J., Teerling, O.J. & Roekaerts, D. (2003). Spectral radiative effects and turbulence/radiation interaction in a non-luminous turbulent jet diffusion flame. *Journal of Geophysical Research*, **133**, 75–91.

Dessler, A.E., Yang, P., Lee, J., Solbrig, J., Zhang, Z. & Minschwaner, K. (1996). Efficient Calculation of Infrred Fluxes and Cooling Rates Using the Two-Stream Equations. *Journal of the Atmospheric Sciences*, **53**, 1921–1932.

Dessler, A.E., Yang, P., Lee, J., Solbrig, J., Zhang, Z. & Minschwaner, K. (2008). An analysis of the dependence of clear-sky top-of-atmosphere outgoing longwave radiation on atmospheric temperature and water vapor. *Journal of Geophysical Research*, **113**, 2139–2156.

Ellingson, R.G., Ellis, J. & Fels, S. (1991). The Intercomparison of Radiation Codes Used in Climate Models: Long Wave Results. *Journal of Geophysical Research*, **96**, 8929–8953.

Fomin, B.A. (2004). A k-distribution technique for radiative transfer simulation in inhomogeneous atmosphere: 1. FKDM, fast k-distribution model for the longwave. *Journal of Geophysical Research*, **109**.

Fu, Q. & Liou, N. (1992). On the Correlated k-Distribution Method for Radiative Transfer in Nonhomogeneous Atmospheres. *Journal of the Atmospheric Sciences*, **49**, 2139–2156.

Hogan, R.J. (2010). The Full-Spectrum Correlated-k Method for Longwave Atmospheric Radiative Transfer Using an Effective Planck Function. *Journal of Atmospheric Sciences*, **67**, 2086–2100.

Jacobson, M.Z. (2004). A Refined Method of Parameterizing Absorption Coefficients among Multiple Gases Simultaneously from Line-by-Line Data. *Jounal of the Atmospheric Sciences*, **62**, 506–517.

Lacis, A.A. & Oinas, V. (1991). A Description of the Correlated k Distribution Method for Modeling Nongray Gaseous Absorption, Thermal Emission, and Multiple Scattering in Vertically Inhomogeneous Atmospheres. *Journal of Geophysical Research*, **96**, 9027–9063.

Li, G. & Modest, M.F. (2002). Application of composition PDF methods in the investigation of turbulenceradiation interactions. *Journal of Quantitative Spectroscopy Radiative Transfer*, **73**, 461472.

Liou, K.N. (1992). *Radiation and Cloud Processes in the Atmosphere*. Oxford Uiversity Press, Oxford.

Mlawer, E., Traubman, S. & Clough, S. (1995). A Rapid Radiative Transfer Model. *Proceedings of the Fifth Atmospheric Radiation Measurement (ARM) Science Team Meeting*, 219–222.

Mlawer, E.J., Taubman, S.J., Brown, P.D., Iacono, M.J. & Clough, S.A. (1997). Radiative transfer for inhomogeneous atmospheres: RRTM, a validated correlated-k model for the longwavel. *Journal of Geophysical Research*, **102**, 16,663–16,682.

Modest, M.F. & Zhang, H. (2002). The Full-Spectrum Correlated-k Distribution for Thermal Radiation From Molecular Gas-Particulate Mixtures. *Journal of Heat Transfer*, **124**, 30–38.

Natraja, V., Jianga, X., Shiaa, R., Huangb, X., Margolisc, J.S. & Yunga, Y.L. (2005). Application of principal component analysis to high spectral resolution radiative transfer: A case study of the O_2 A band. *Journal of Quantitative Spectroscopy Radiative Transfer*, **95**, 539556.

Oinas, V., Lacis, A.A., Rind, D., Shindella, D.T. & Hansen, J.E. (2001). Radiative cooling by stratospheric water vaporbig differences in GCM results. *Journal of the Atmospheric Sciences*, **28**, 2791–2794.

Pawlak, D.T., Clothiaux, E.E., Modest, M.F. & Cole, J.N.S. (2004). Full-Spectrum Correlated-k Distribution for Shortwave Atmospheric Radiative Transfer. *Journal of the Atmospheric Sciences*, **61**, 2588–2601.

Petty, G.W. (2004). *A First Course in Atmospheric Radiation*. Pitman Research Notes in Mathematics Series, Sundog Publishing, Wisconsin.

Ritter, B. & Geleyn, J.F. (1992). A Comprehensive Radiation Scheme for Numerical Weather Prediction Models with Potential Applications in Climate Simulations. *Monthly Weather Review*, **120**, 303–325.

Stephens, G.L. (1984). The Parameterization of Radiation for Numerical Weather Prediction and Climate Models. *Monthly Weather Review*, **112**, 826–867.

Stull, R.B. (1989). *Boundary Layer Meteorolgoy*. Kluwer Academic Publishers, Netherlands.

Turner, D.D., Tobin, D.C., Clough, S.A., Brown, P.D., Ellingson, R.G., Mlawer, E.J., Knuteson, R.O., Revercomb, H.E., Shippert, T.R., Smith, W.L. & Sheppard, M.W. (2004). The QME AERI LBLRTM: A Closure Experiment for Downwelling High Spectral Resolution Infrared Radiance. *Journal of the Atmospheric Sciences*, **61**, 2657–2675.